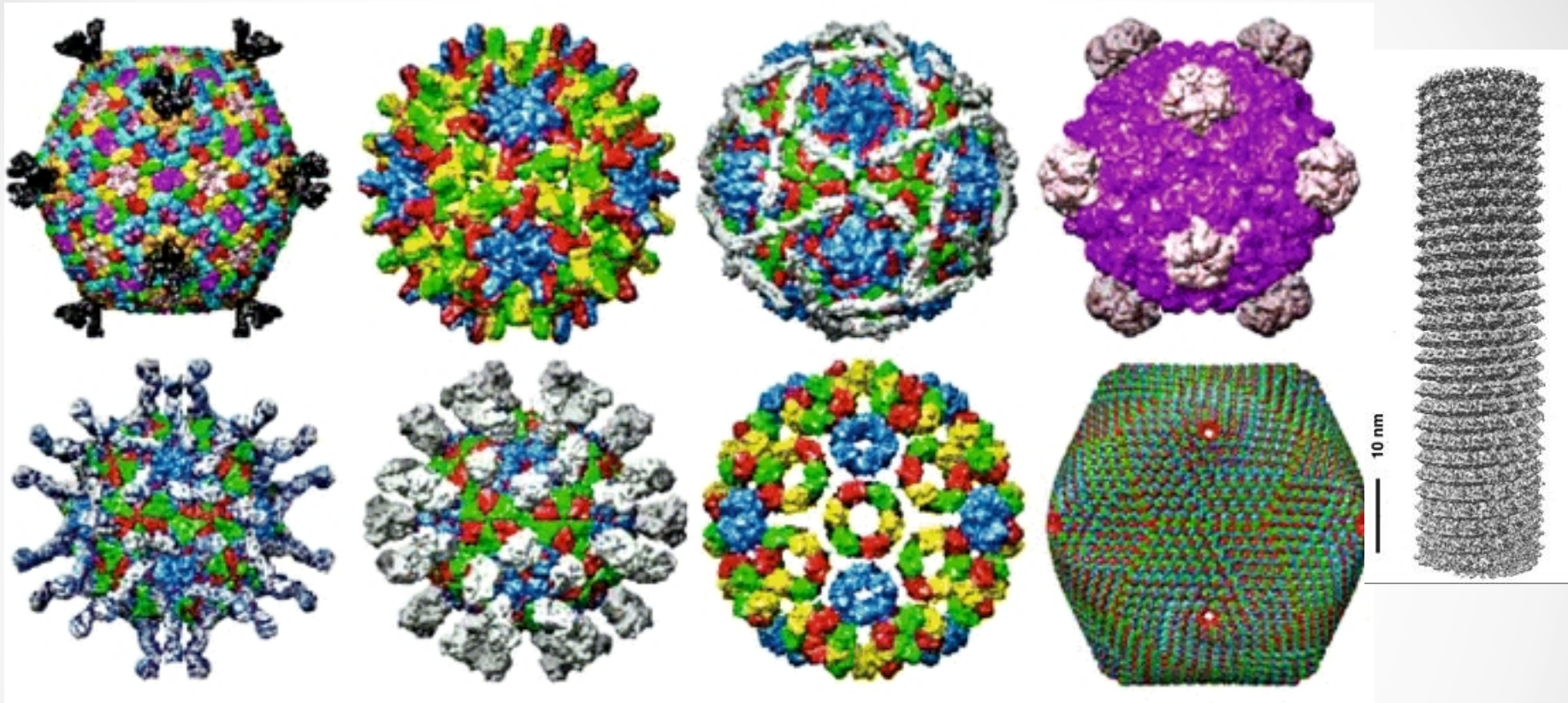


Single particle cryoelectron microscopy and 3D reconstruction of viruses

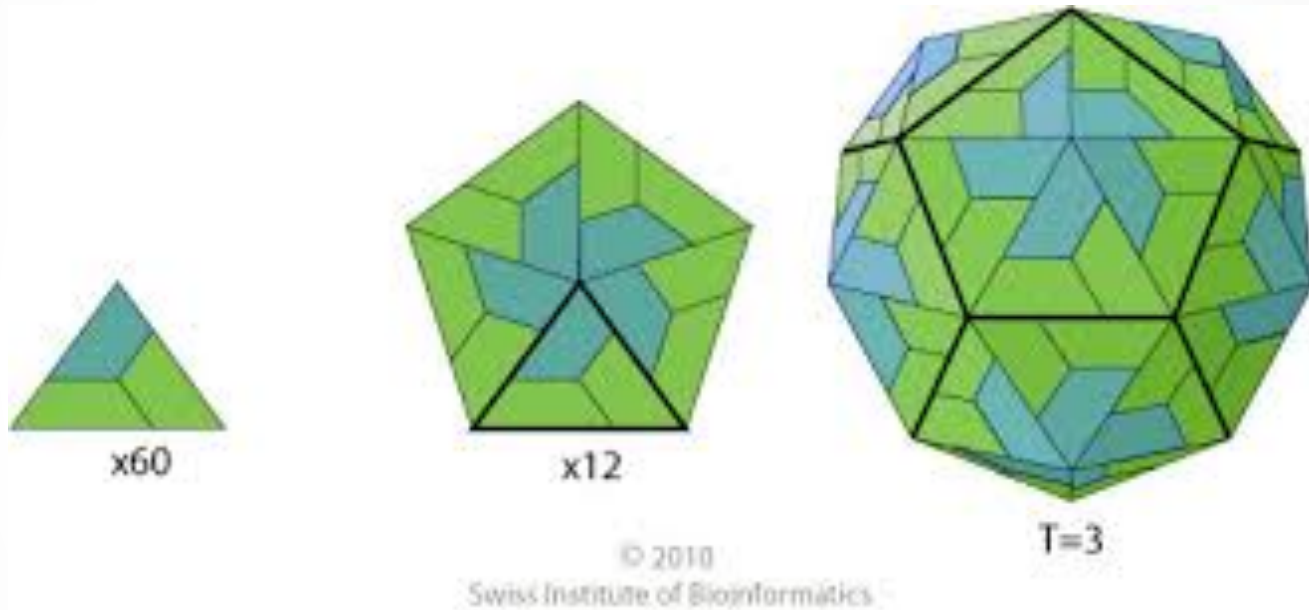
Manidipa Banerjee
Assistant Professor
Indian Institute of Technology, Delhi

Virus Types

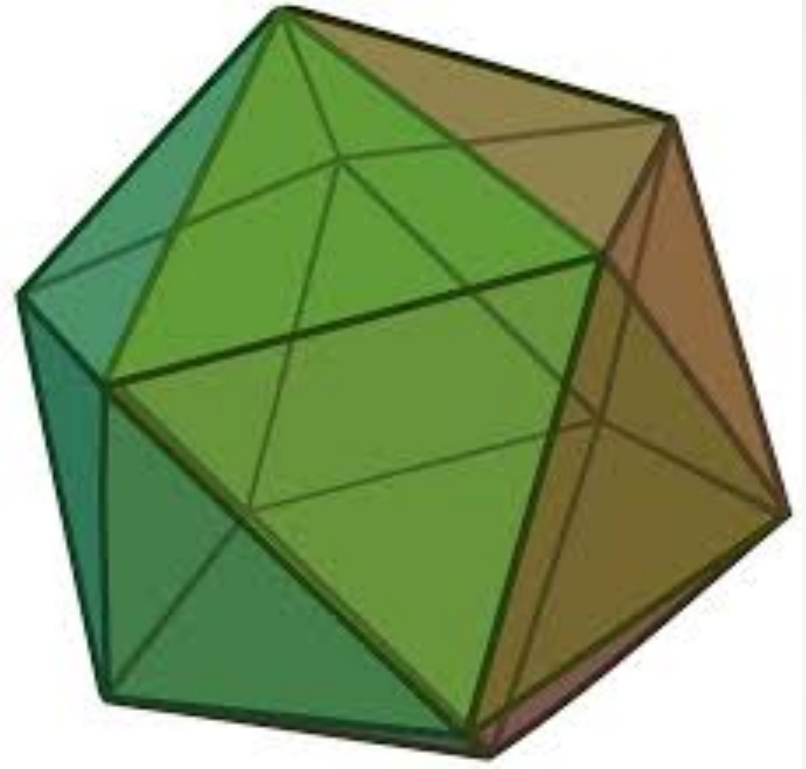
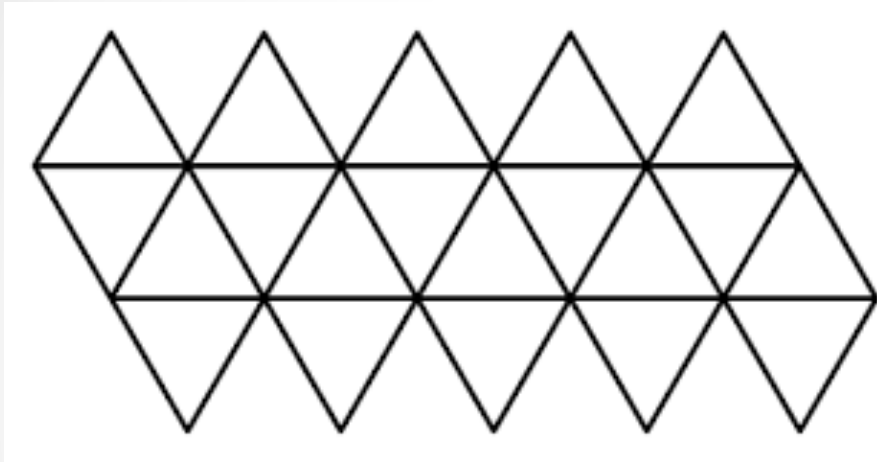


Composed of protein, nucleic acid (ss/ds DNA/RNA) and lipid components
Icosahedral, helical, oblate, head-tail structures
Genome codes for non-structural proteins, scaffolding proteins
Viral genome contributes less mass than viral proteins
Multiple copies make up capsid

Icosahedral organization of virus capsids



Icosahedral organization of virus capsids



Protein tertiary structure is non-symmetric

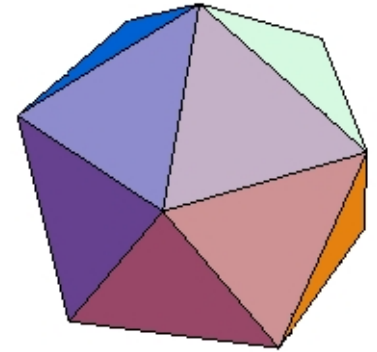
Need to form a stable, closed structure to protect the genome

Minimum free energy = maximum number of intersubunit bonds

Icosahedral organization of virus capsids

Constructed from 20 equilateral triangles

60 subunits form an icosahedron



Requires a greater number of subunits to form a same volume
(size of subunits smaller, less genetic information required)

Physical constraints prevent tight packing of subunits required for tetrahedral and octahedral geometry

Icosahedral organization of virus capsids

Early information from X-ray crystallography

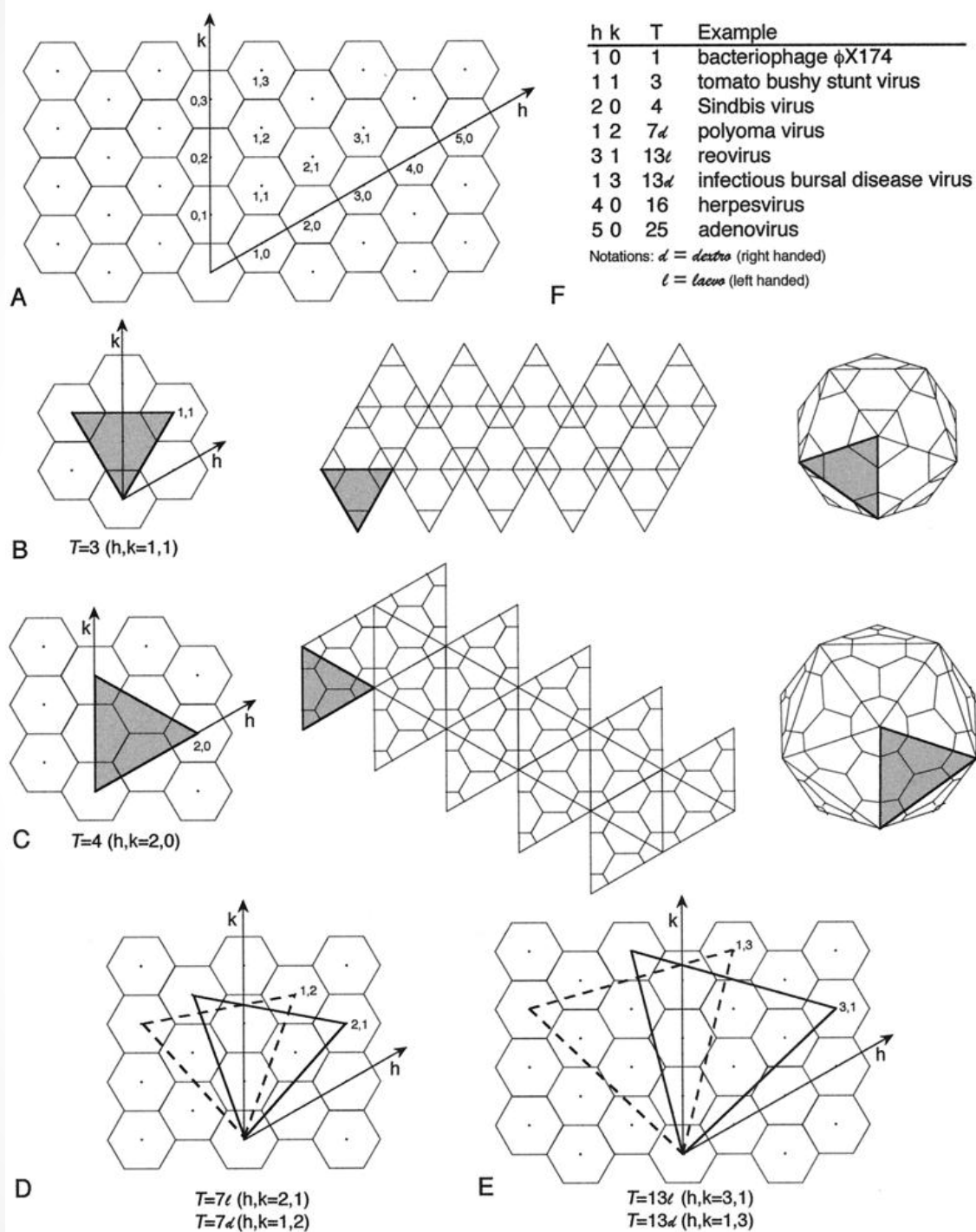
Tomato Bushy Stunt Virus at 2.8 Å: Harrison *et al* (1978)

Southern bean Mosaic Virus at 2.8 Å: Abad-Zapetero *et al* (1980)

Satellite Tobacco Necrosis Virus at 3.0 Å: Liljas *et al* (1982)

•
•
•
•

Adenovirus at 3.5 Å: Reddy *et al* (2010)



Icosahedral organization of virus capsids

Minimum of 60 subunits required

>60 subunits accommodated by expansion of triangular facets, and subdivision

Triangulation number

$$T = H^2 + HK + K^2$$

Three classes:

$$H \geq 1, K = 0 \text{ (} T=1, 4, 9, \dots \text{)}$$

$$H = K \geq 1 \text{ (} T= 3, 12, 27, \dots \text{)}$$

$H \neq K \geq 1$ ($T = 7, 13, 19, 21, \dots$) skewed class, leavo or dextro enantiomorphic configurations

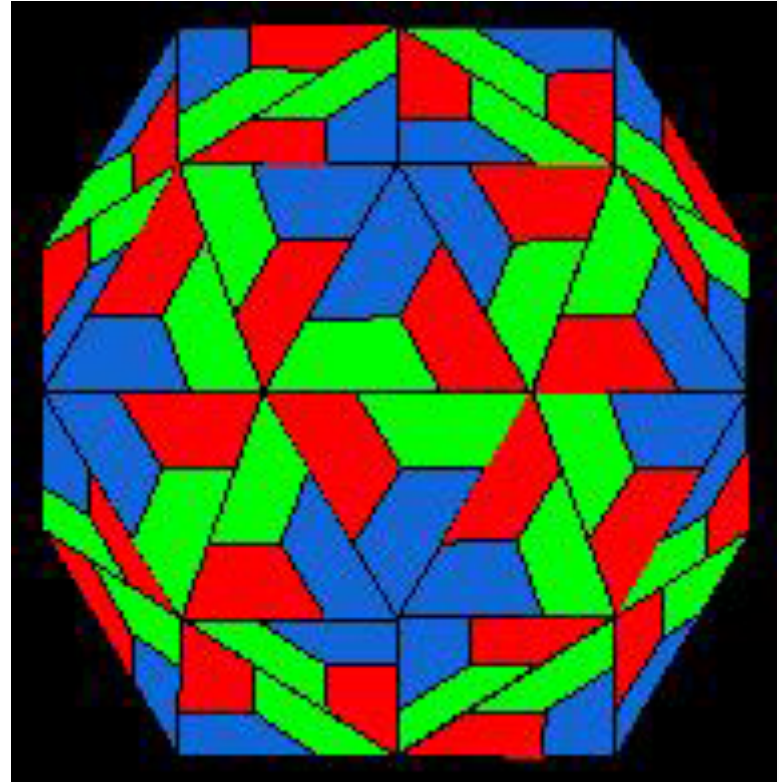
Polyomavirus ($T=7d$), Rotavirus ($T = 13l$)

Icosahedral organization of virus capsids

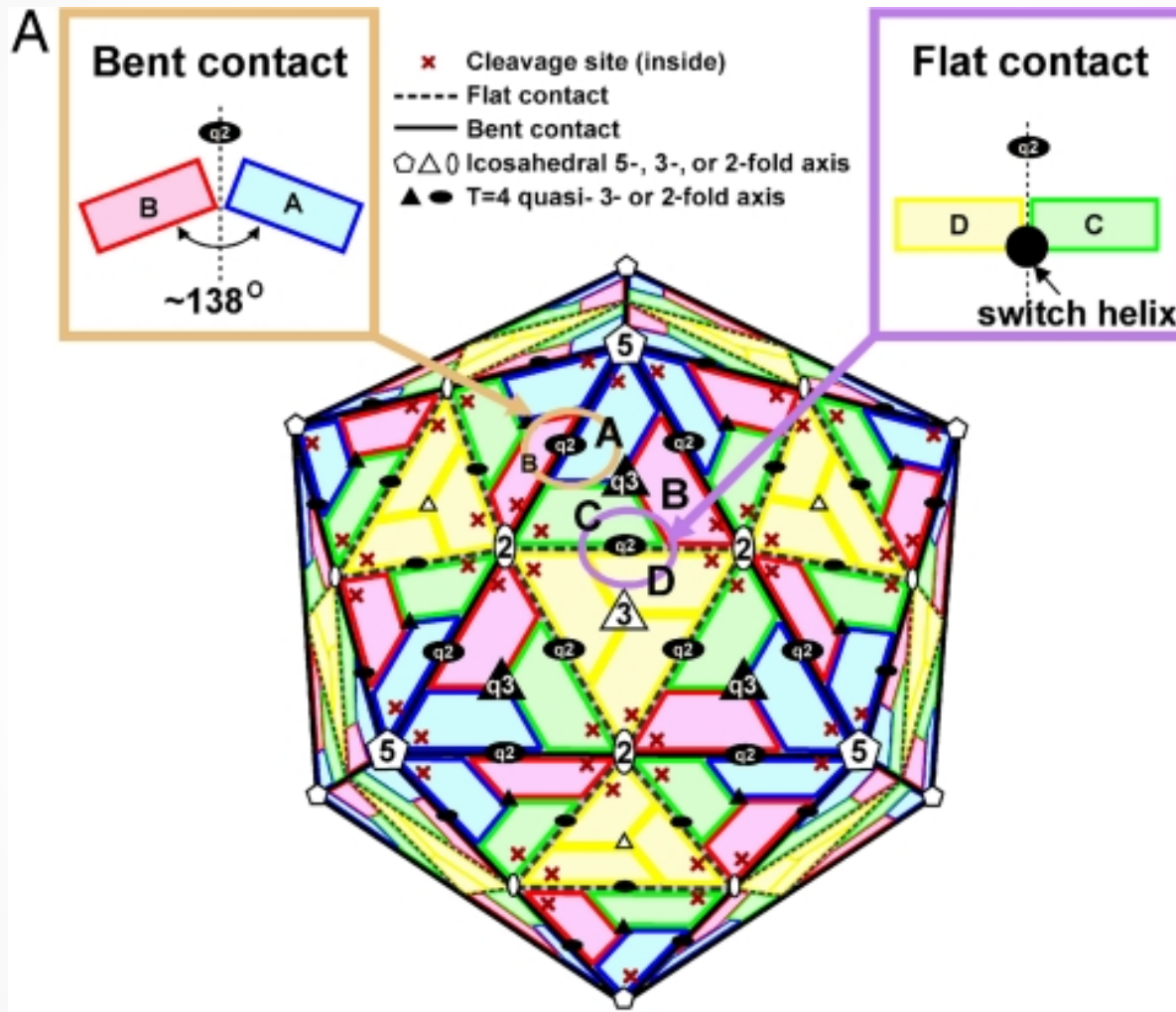
Icosahedral asymmetric unit (iASU)

Quasi-equivalence of subunits

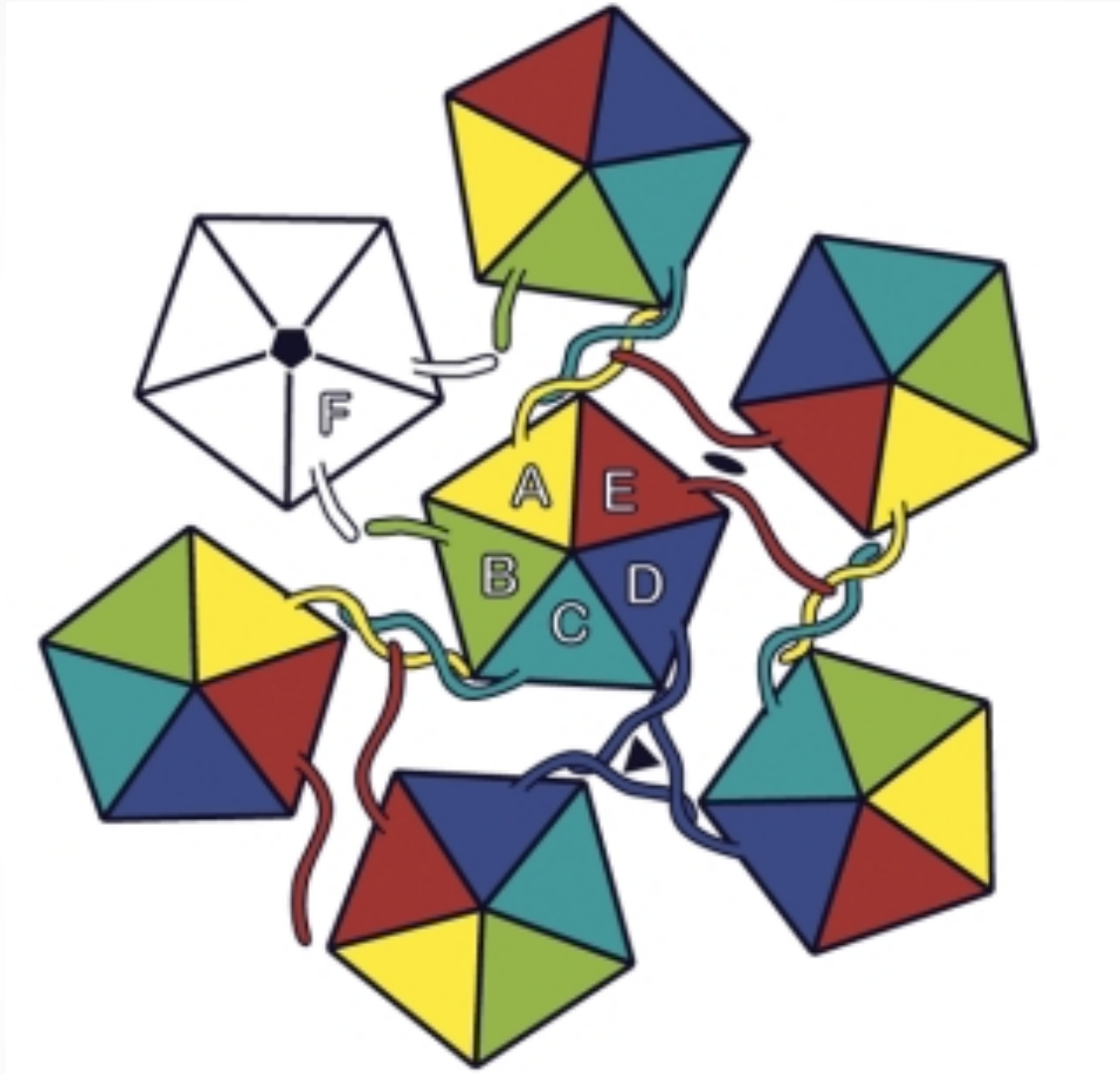
12 pentamers, 10 (T-1) hexamers



Icosahedral organization of virus capsids



Departure from icosahedral organization



Bovine papillomavirus: 72 pentamers

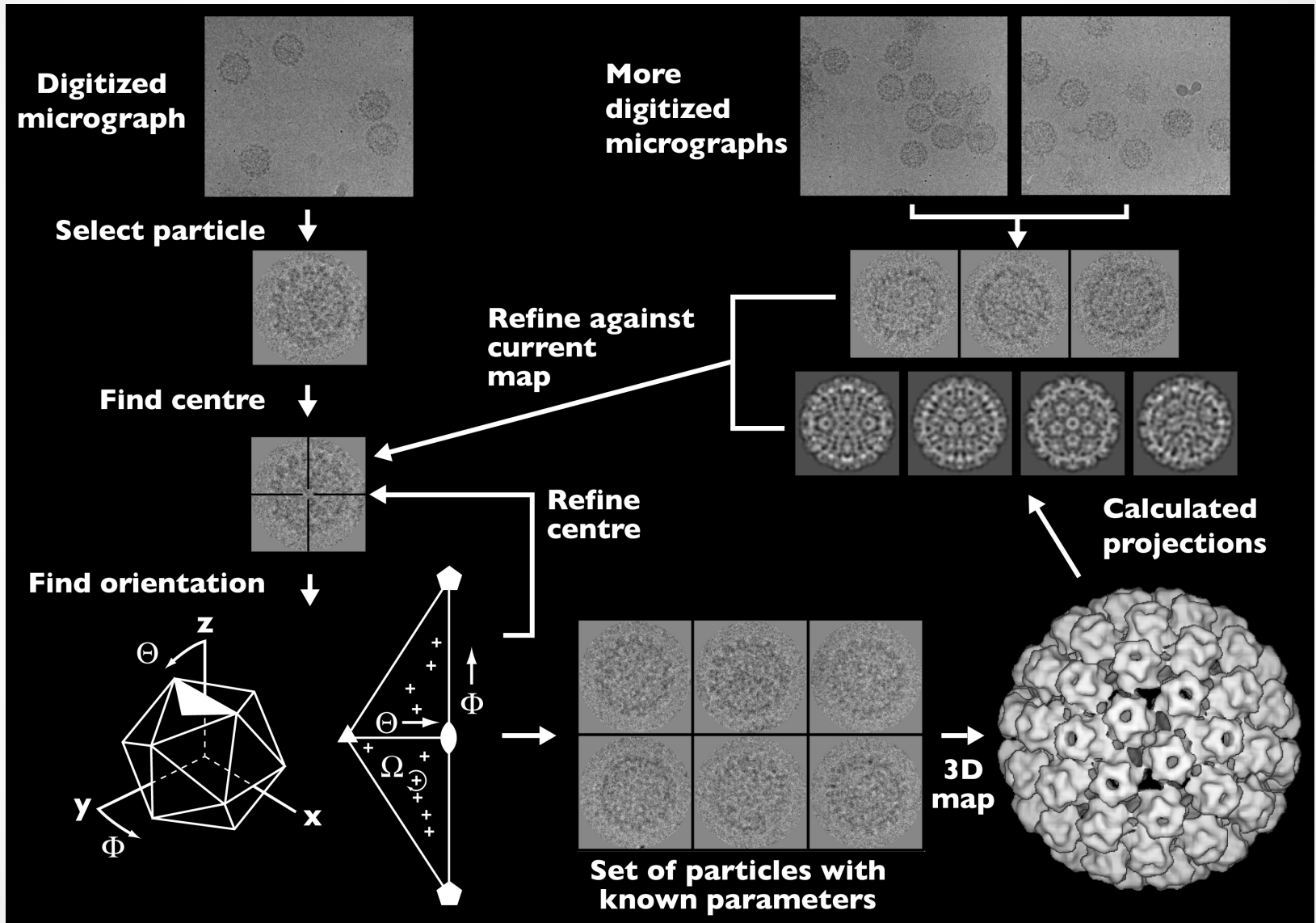
Departure from icosahedral organization



Adenovirus

240 trimers occupy hexavalent positions

Cryoelectron microscopy and 3D reconstruction of icosahedral viruses



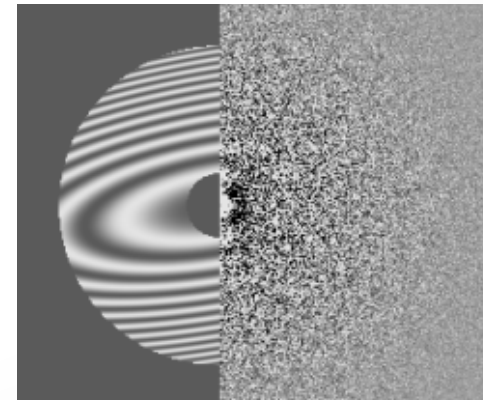
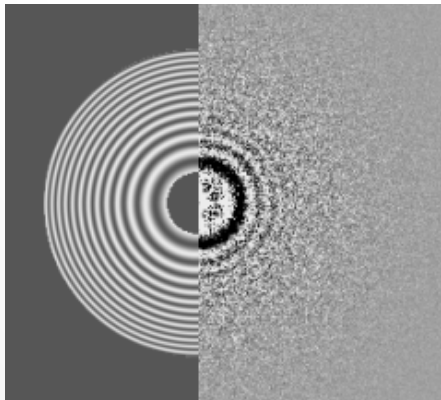
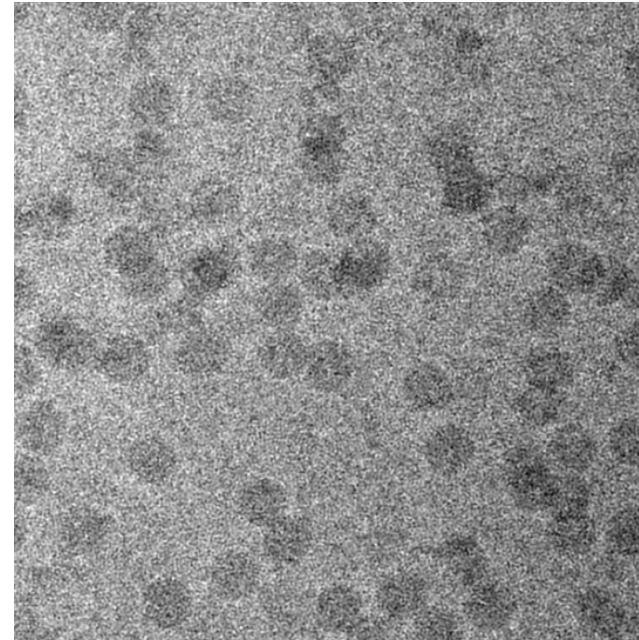
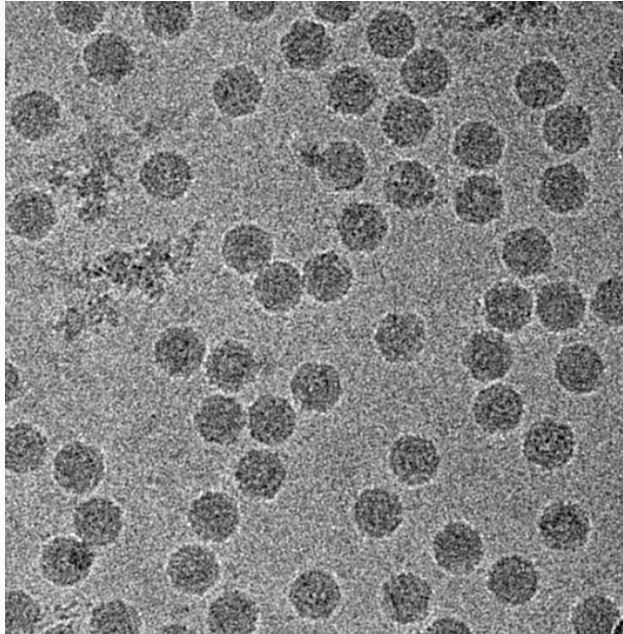
Cryoelectron microscopy and 3D reconstruction of icosahedral viruses

Negatively stained Tomato Bushy Stunt Virus

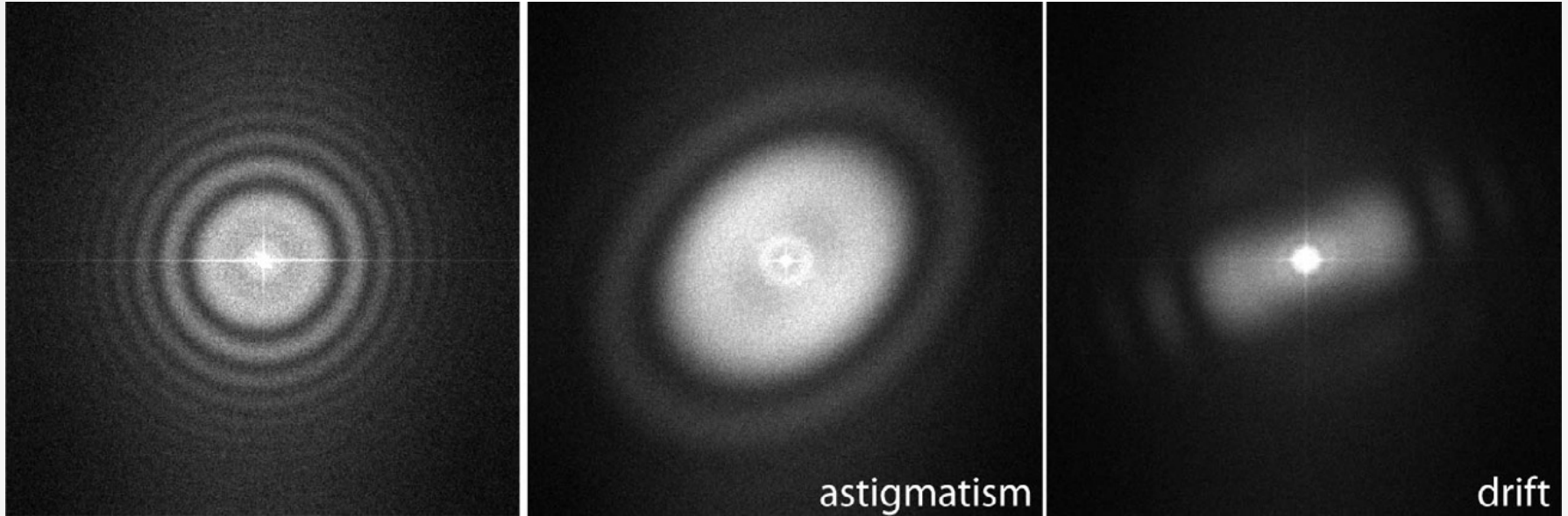
Common lines to find the orientations of 2D particles

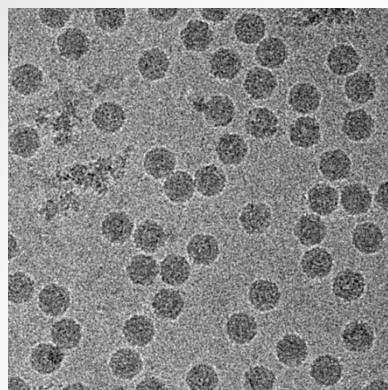
Fourier Bessel method to compute 3D map

Cryoelectron microscopy and 3D reconstruction of icosahedral viruses

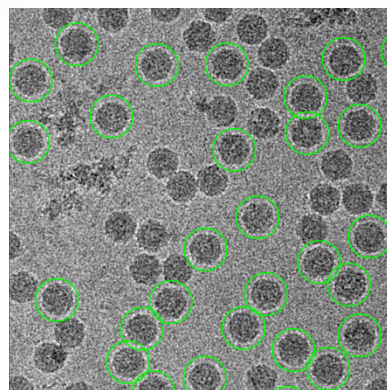


Cryoelectron microscopy and 3D reconstruction of icosahedral viruses

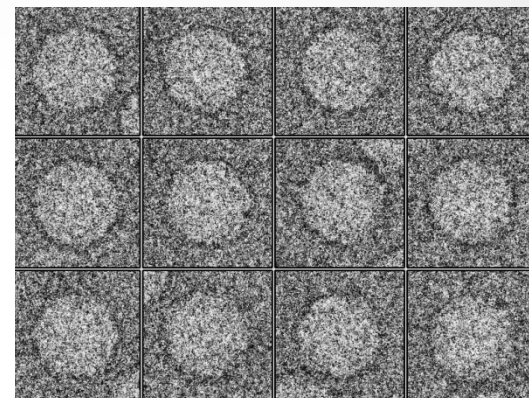




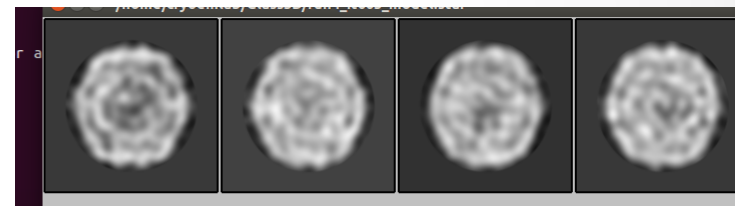
Data Collection



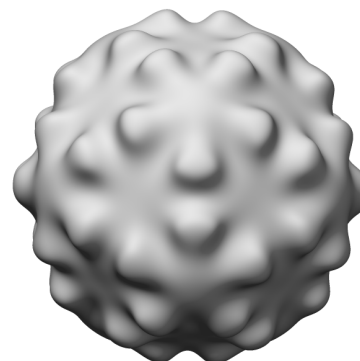
Particle
Extraction



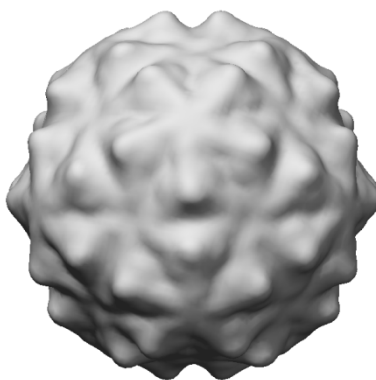
Boxing



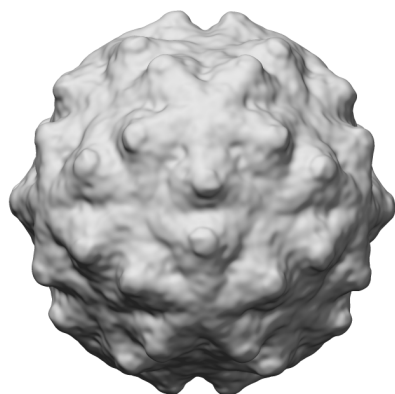
2D Classification



Initial Model
Generation



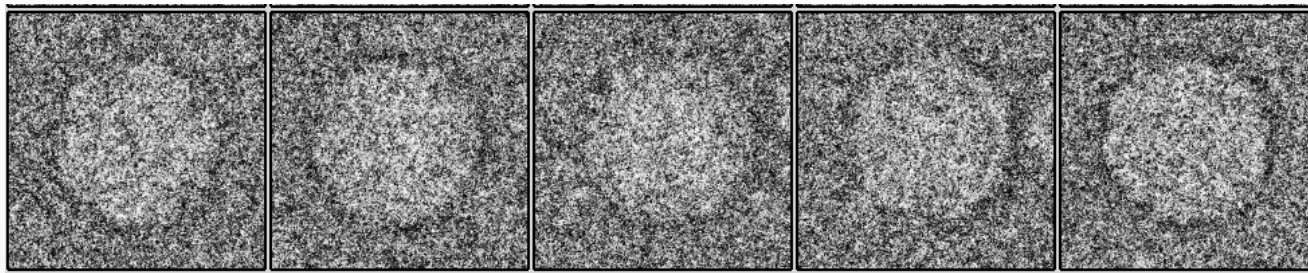
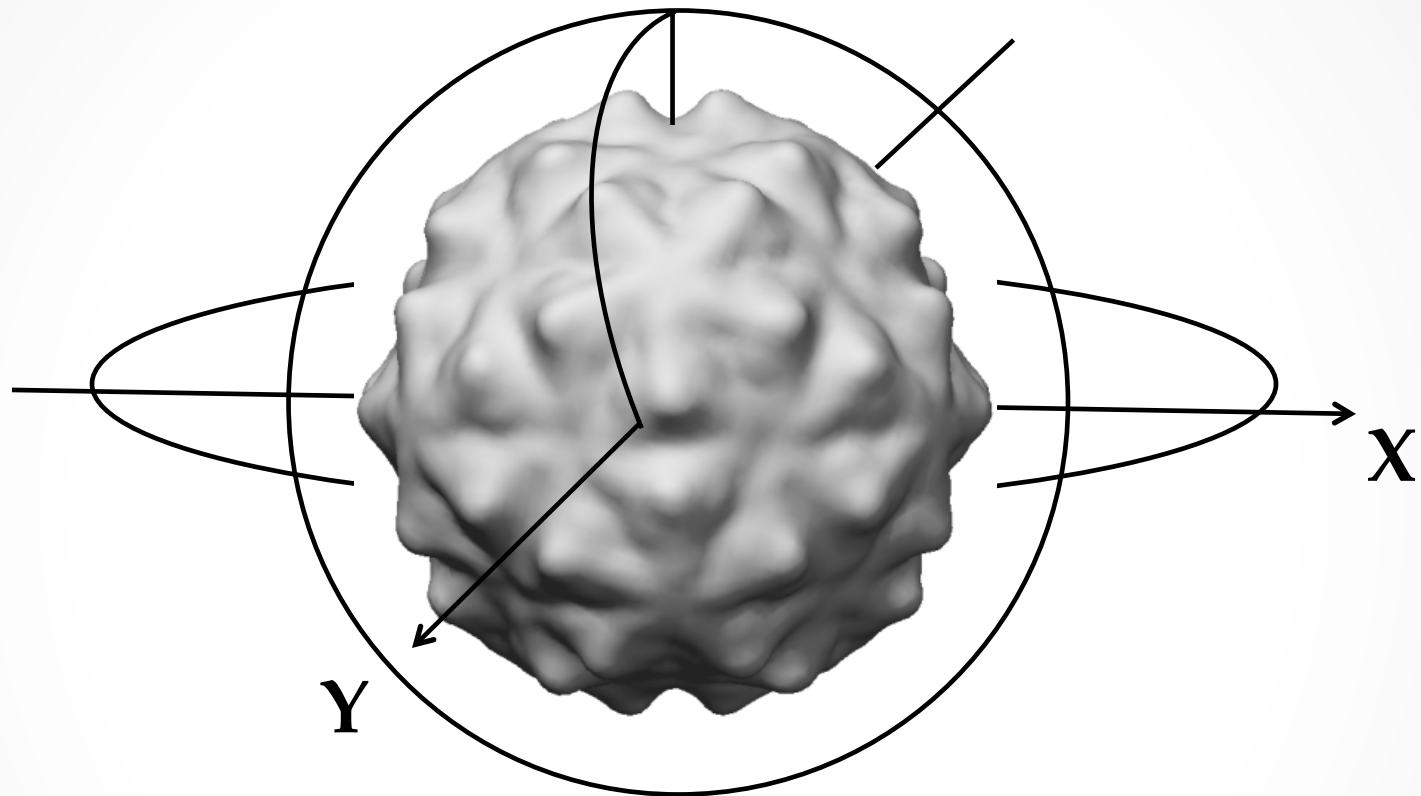
3D Model



Refinement

Steps in 3D reconstruction

Cryoelectron microscopy and 3D reconstruction of icosahedral viruses



A

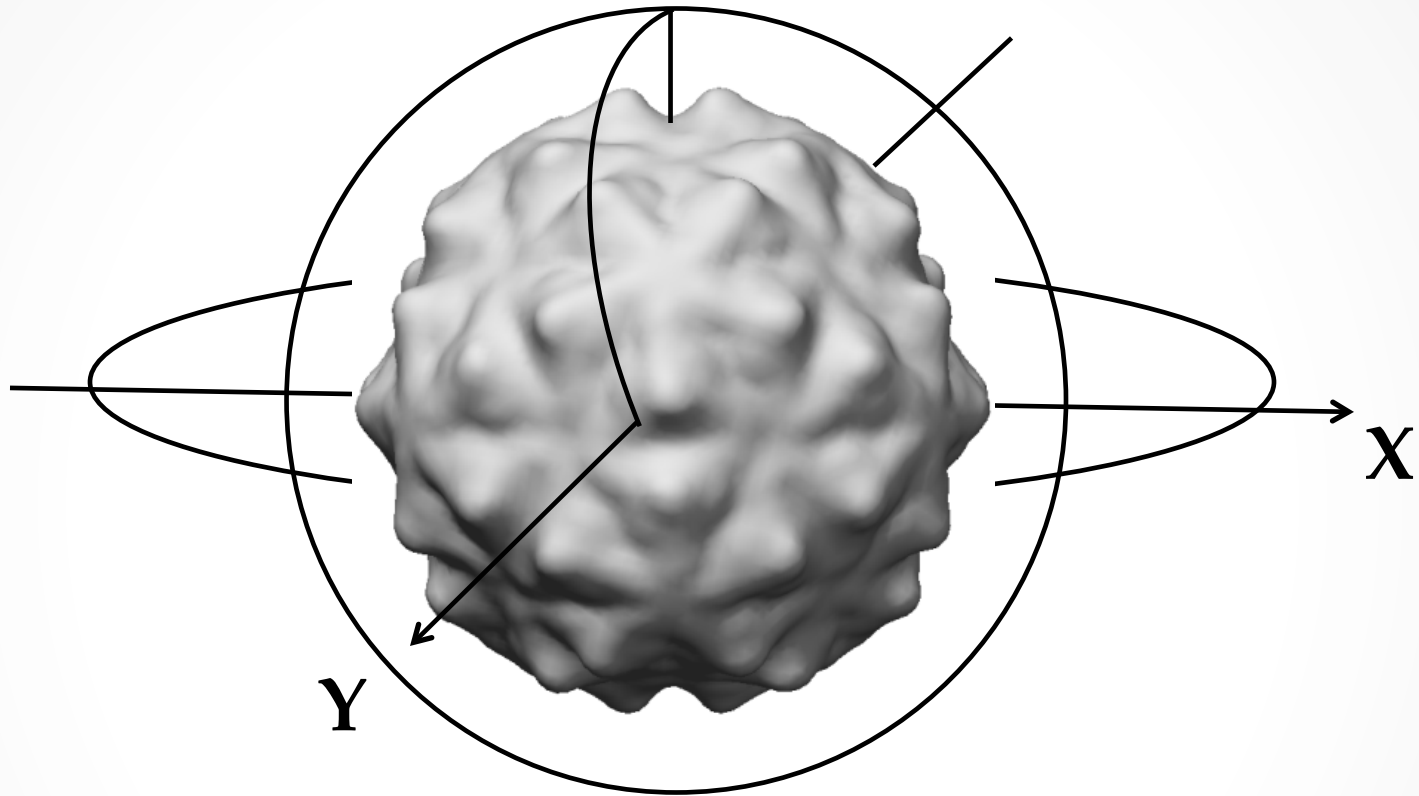
A

A

A

A

Cryoelectron microscopy and 3D reconstruction of icosahedral viruses



Assignment of 5 spatial parameters to each image:
 $x, y, \theta, \Phi, \omega$

Cryoelectron microscopy and 3D reconstruction of icosahedral viruses

How to generate an initial model?

- 1) Download a density map from EMDB, scale dimensions, filter to keep only icosahedral features
- 2) Randomly assign icosahedral orientations to a few hundred particles, generate model from raw data
- 3) Compute self-common lines for a few images, no reference model required

Good data minimizes possibilities of model bias

Cryoelectron microscopy and 3D reconstruction of icosahedral viruses

Particle orientation and center determination

Projection matching and class averages

Determine particle's projection angles (θ , Φ), in-plane rotation angle (ω), center (x , y)

Projections matched with particle images

2D class averaging

Cryoelectron microscopy and 3D reconstruction of icosahedral viruses

Particle orientation and center determination

Common lines method

60 equivalent icosahedral orientations: each define a plane in Fourier space

The line at which any two planes intersect is a self-common line

37 self common lines for any icosahedral particle

Particle's center should be identified correctly

No model required

Cross-common lines: between two particles

Cryoelectron microscopy and 3D reconstruction of icosahedral viruses

Reconstructing a 3D volume

1) Fourier space reconstructions

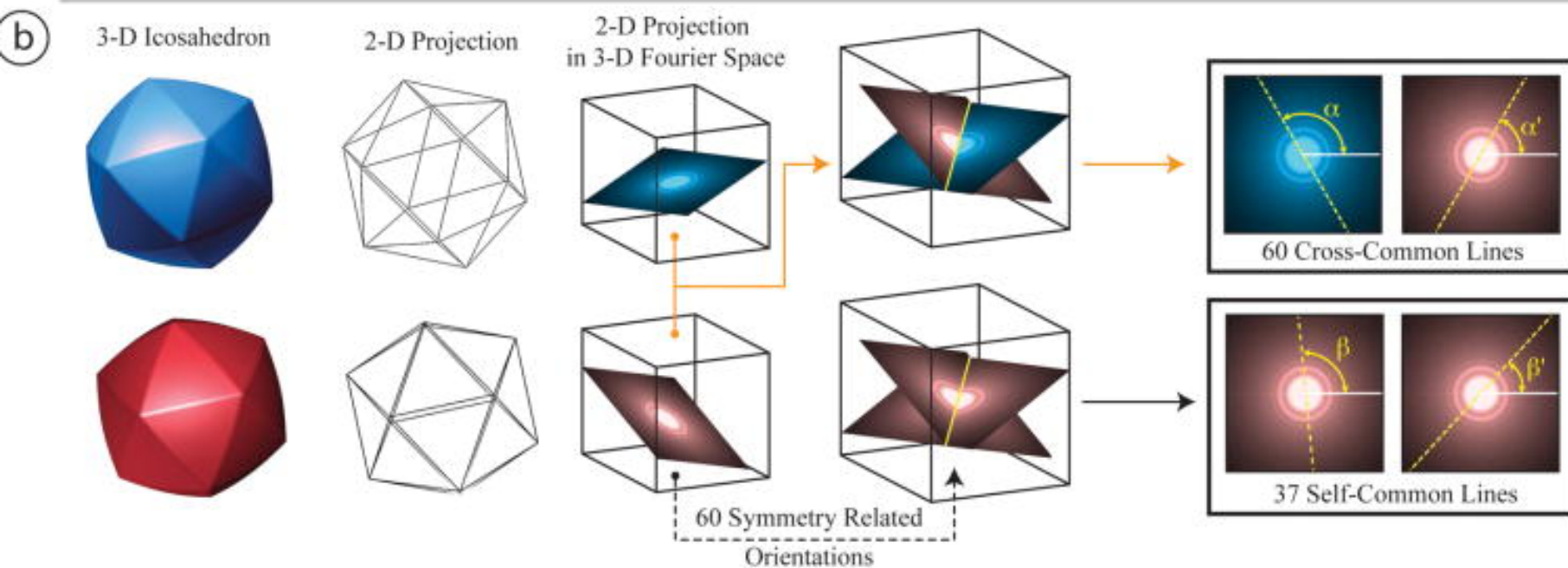
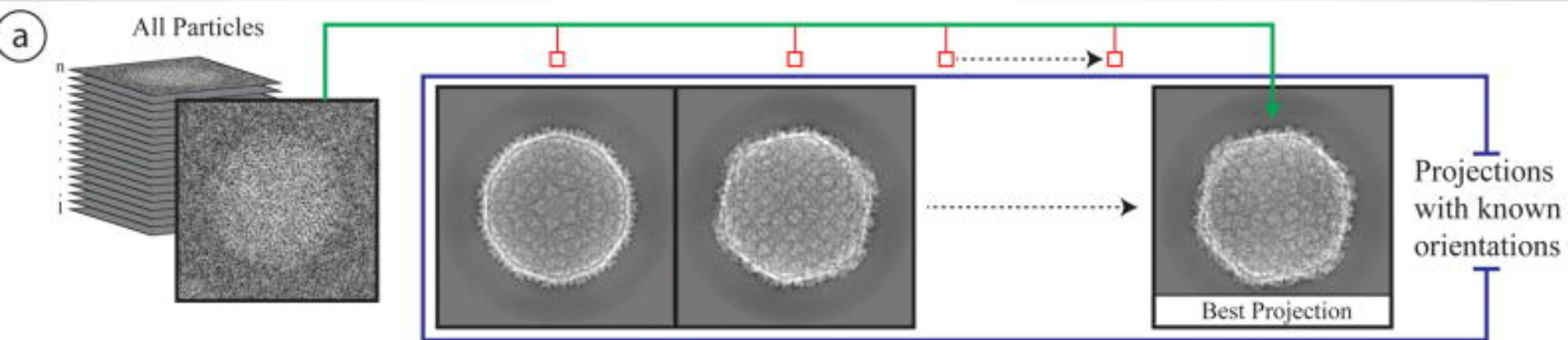
Central section theorem

2D FTs inserted into 3D matrix, based on particle spatial parameters

2) Real space reconstructions

Back projection

Non-crystallographic symmetry averaging: Extracting and averaging similar subunits



Cryoelectron microscopy and 3D reconstruction of icosahedral viruses

Symmetry-free reconstructions

Density for asymmetric/less symmetric regions blurred out

60-fold more images required

Optimization of SNR of asymmetric regions

Defocus/phase plate

Cryoelectron microscopy and 3D reconstruction of icosahedral viruses

How to generate a model for symmetry-free reconstructions?

Low-pass filtering an equivalent structure

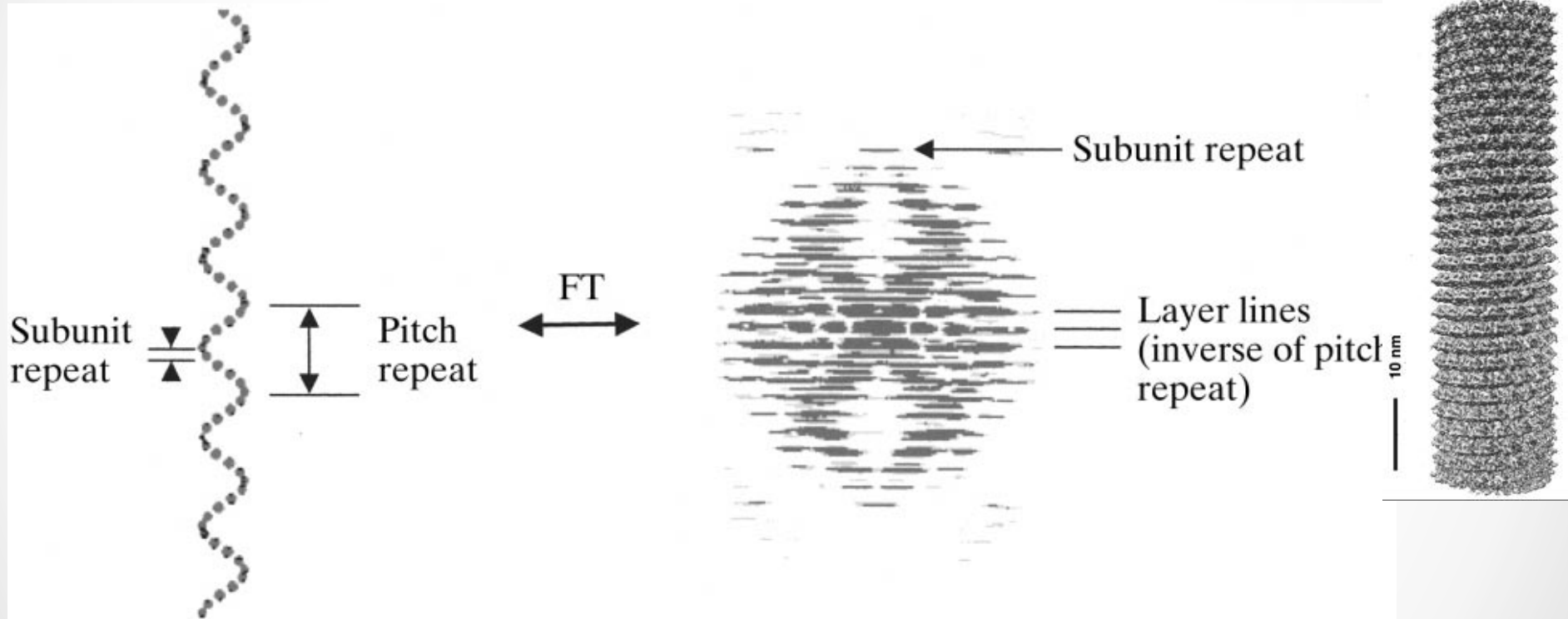
Geometric shape mimicking the component

Extracting shape information by lowering icosahedral threshold of entire map

Orientation assignment, 3D reconstruction

Cryoelectron microscopy and 3D reconstruction of icosahedral viruses

Helical reconstruction



Cryoelectron microscopy and 3D reconstruction of icosahedral viruses

Helical reconstruction

No of equivalent views a function of length of helix and number of units per helical repeat

In ideal situation, a single image is sufficient for a reconstruction

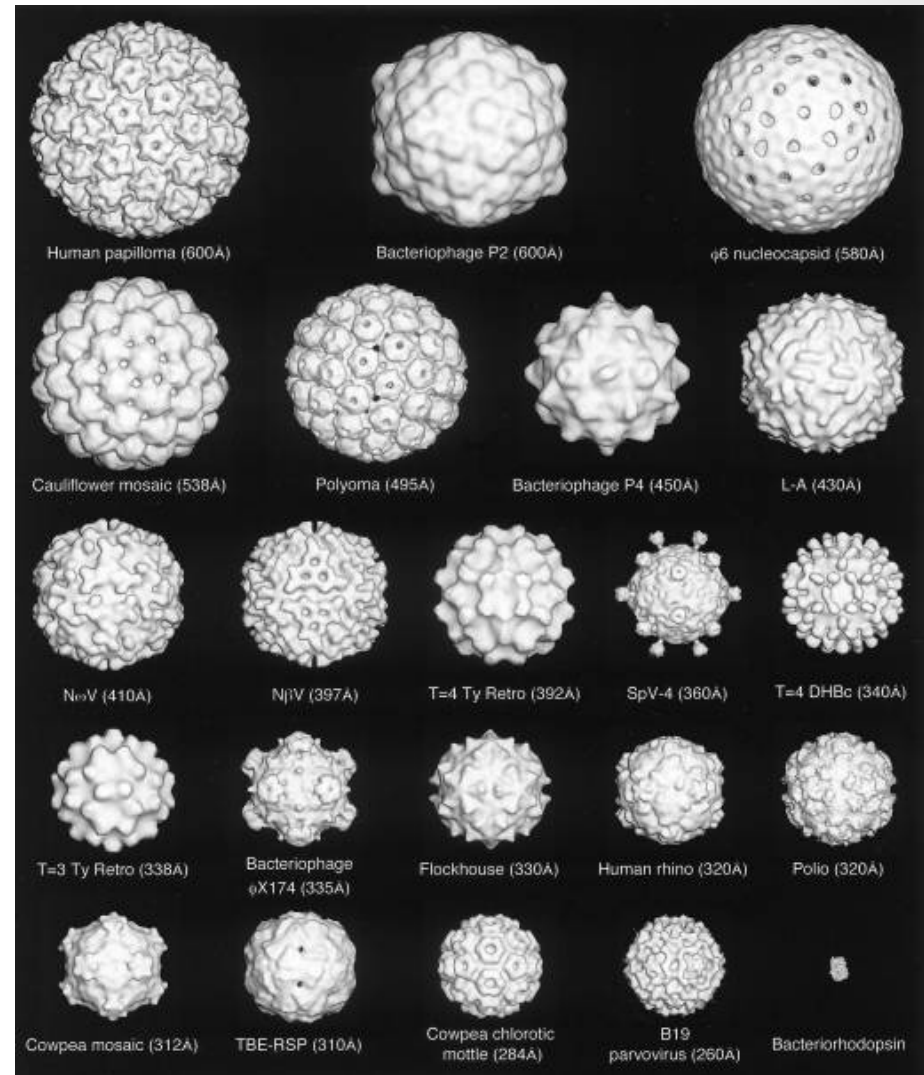
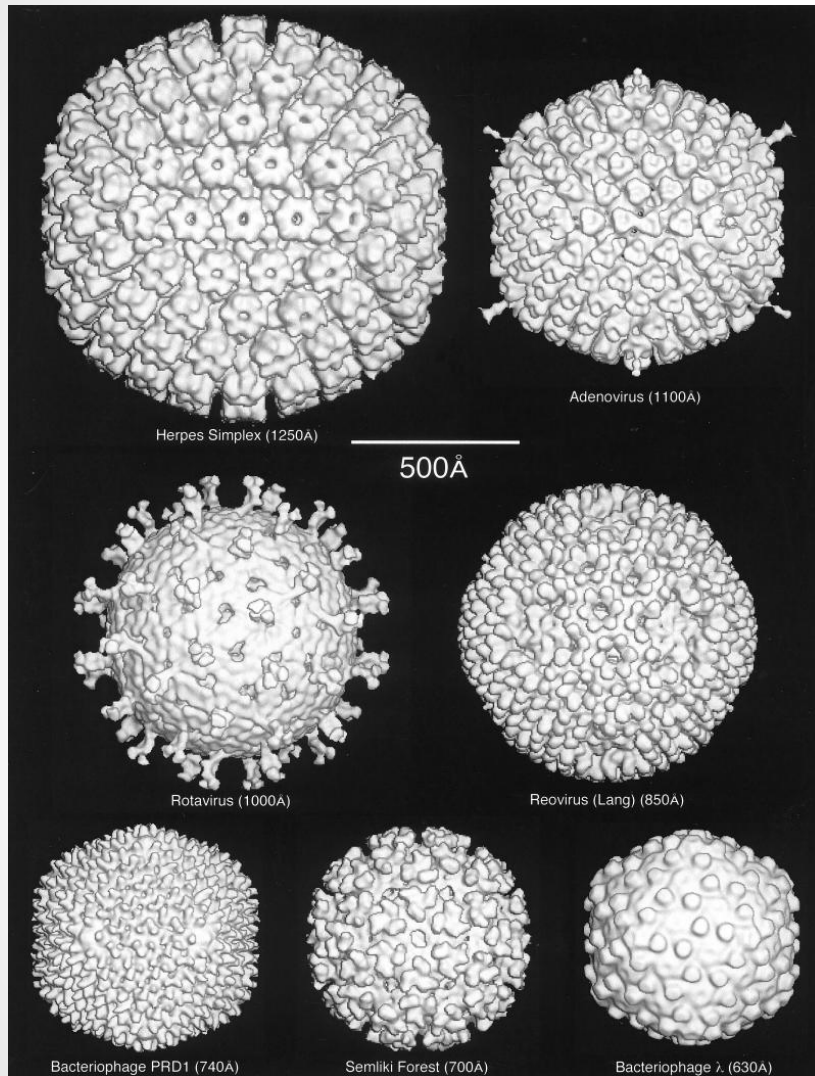
In reality, all helices distorted

Images of helical fragments divided into short, overlapping segments

Segments aligned as separate images based on projection matching

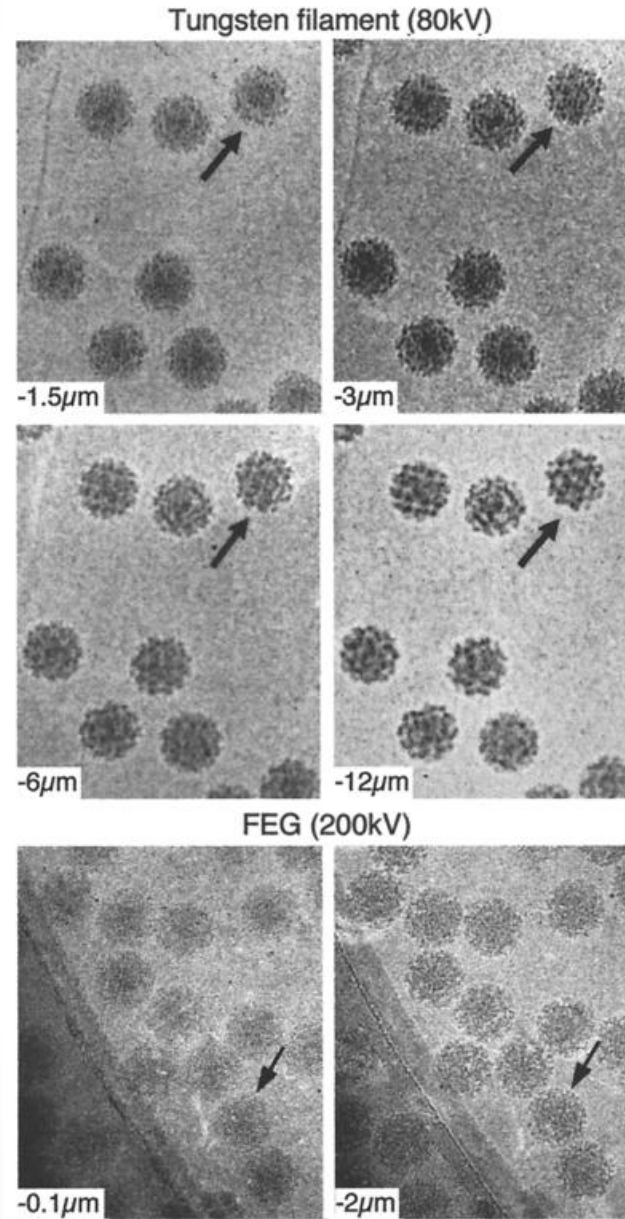
Minimization of differences between symmetry-related elements

Cryoelectron microscopy and 3D reconstruction of icosahedral viruses

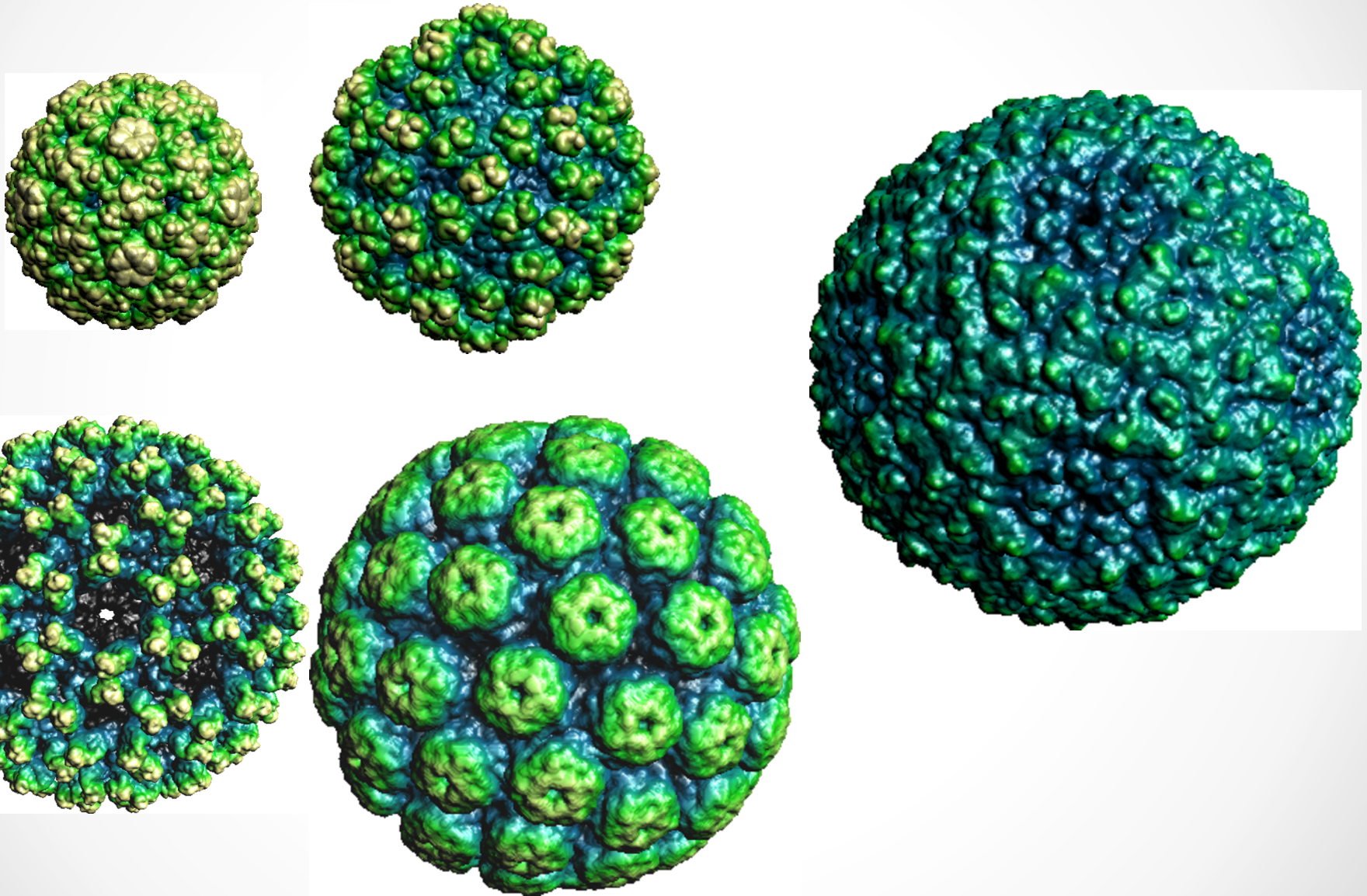


Baker *et al.*, Microbiol Mol Biol Rev, 1999

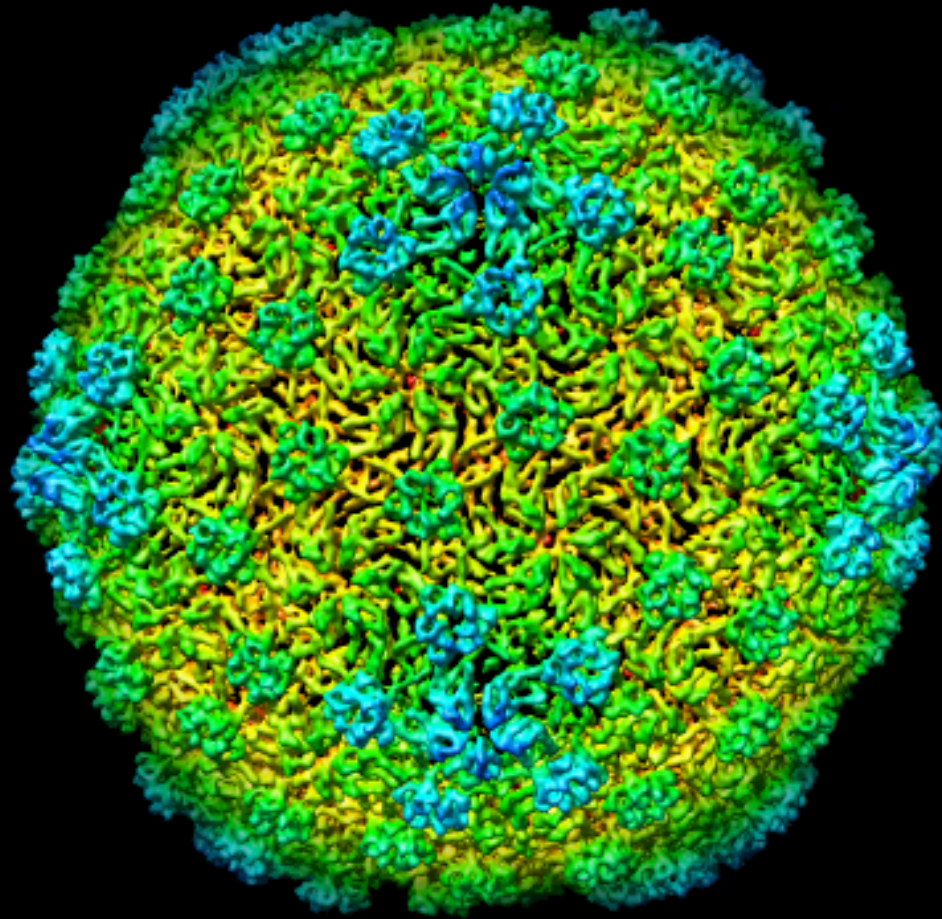
Cryoelectron microscopy and 3D reconstruction of icosahedral viruses



Cryoelectron microscopy and 3D reconstruction of icosahedral viruses

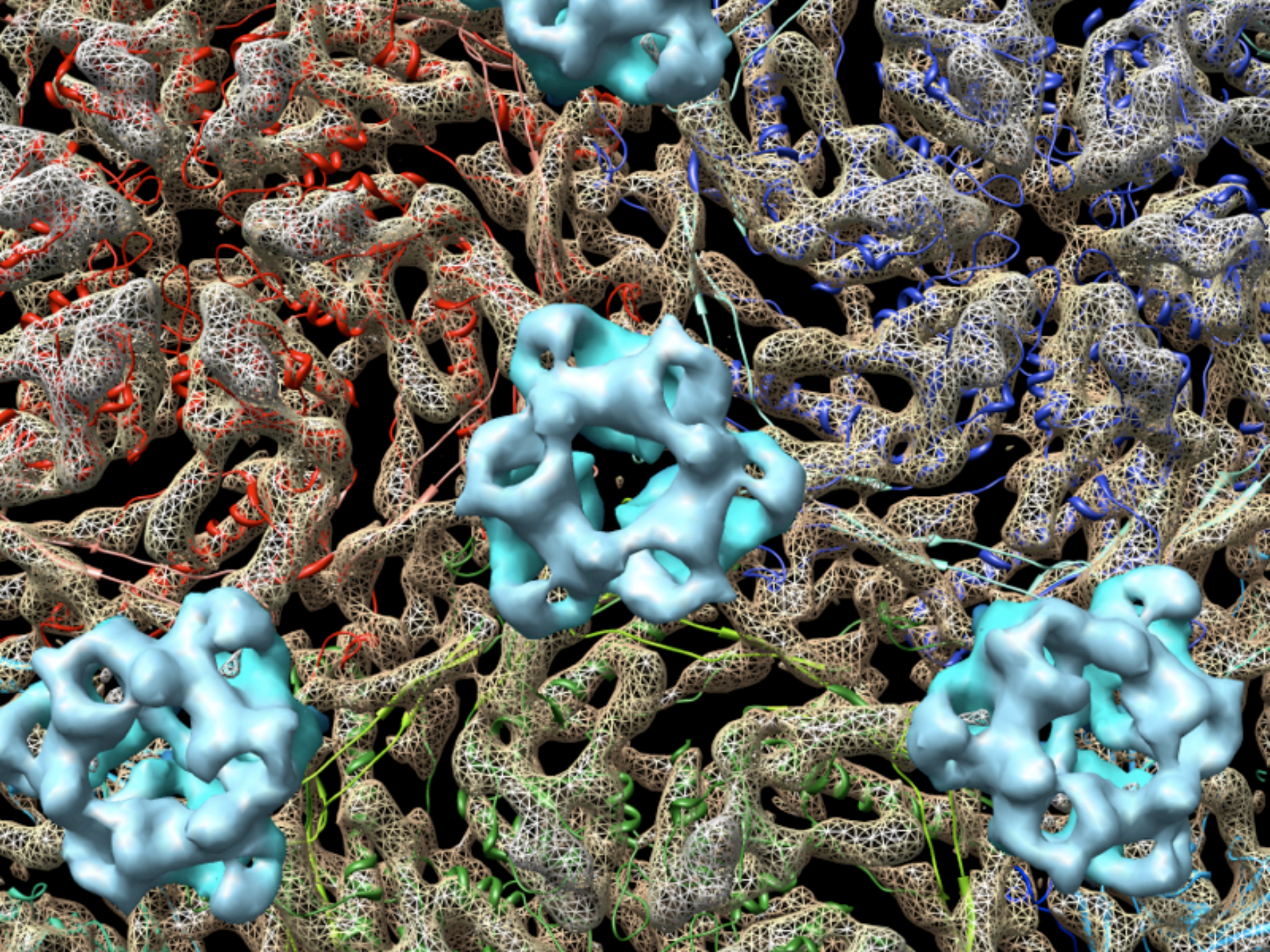


Cryoelectron microscopy and 3D reconstruction of icosahedral viruses

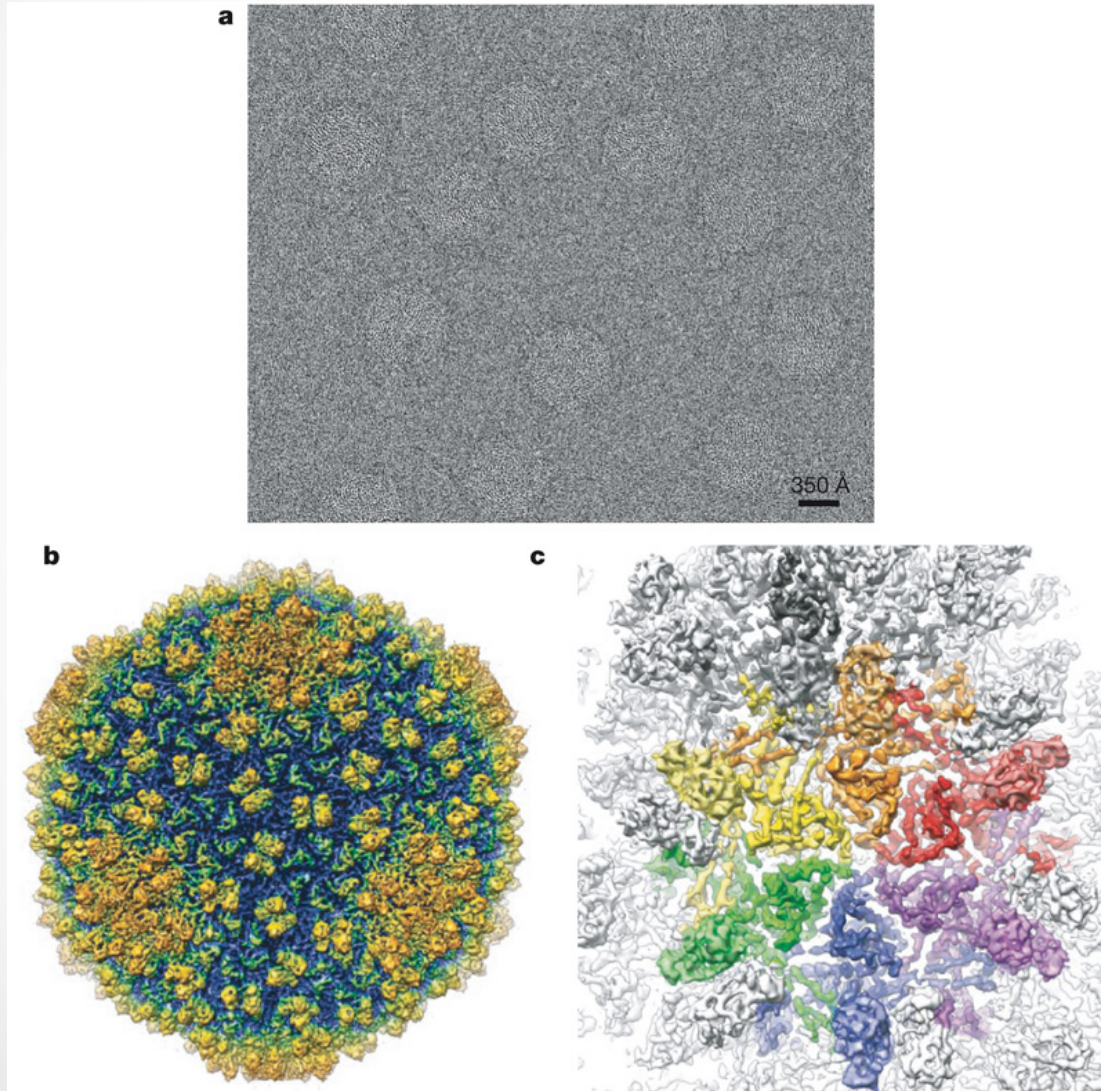


Subnanometer
structures

Lambda phage
stabilization by gpL



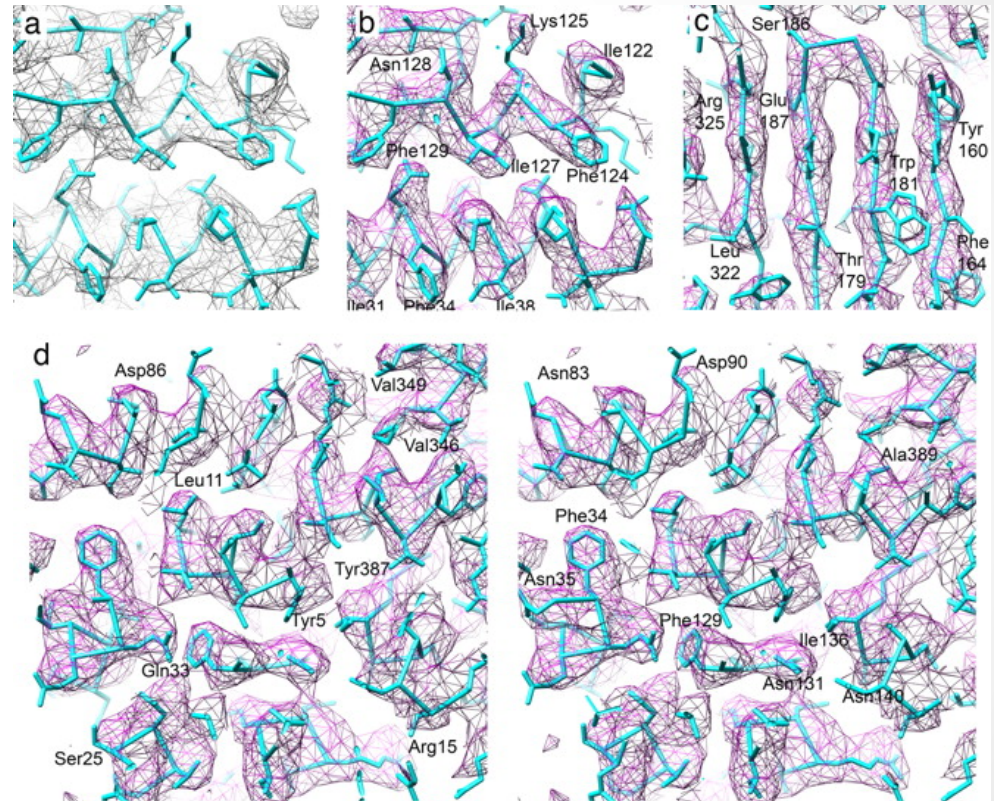
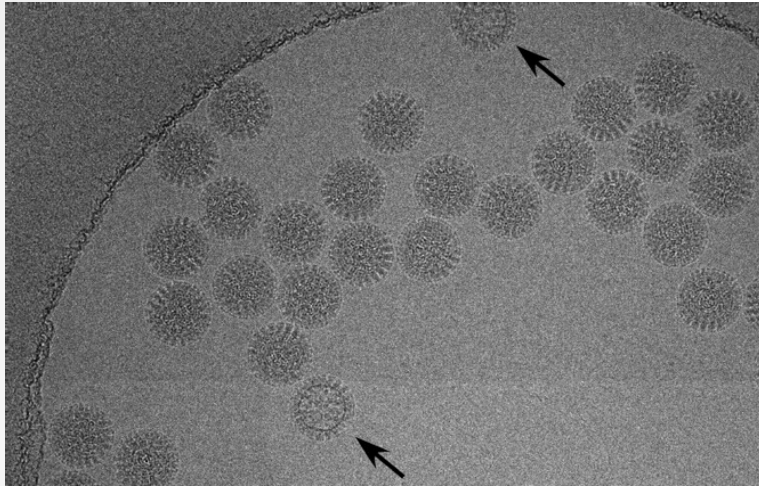
Cryoelectron microscopy and 3D reconstruction of icosahedral viruses



Epsilon15 virus at 4.5 Å

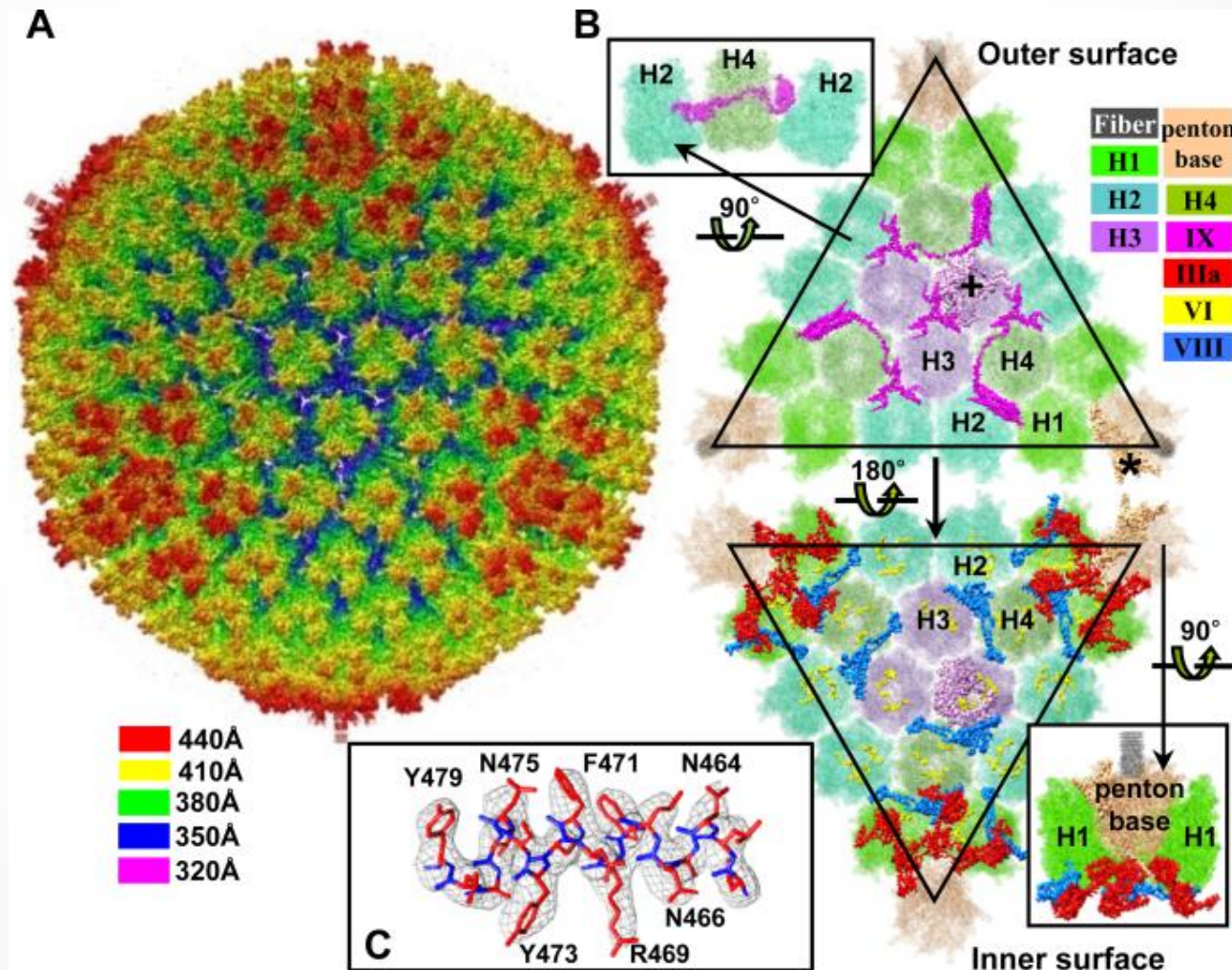
Cryoelectron microscopy and 3D reconstruction of icosahedral viruses

Rotavirus at 3.5 Å

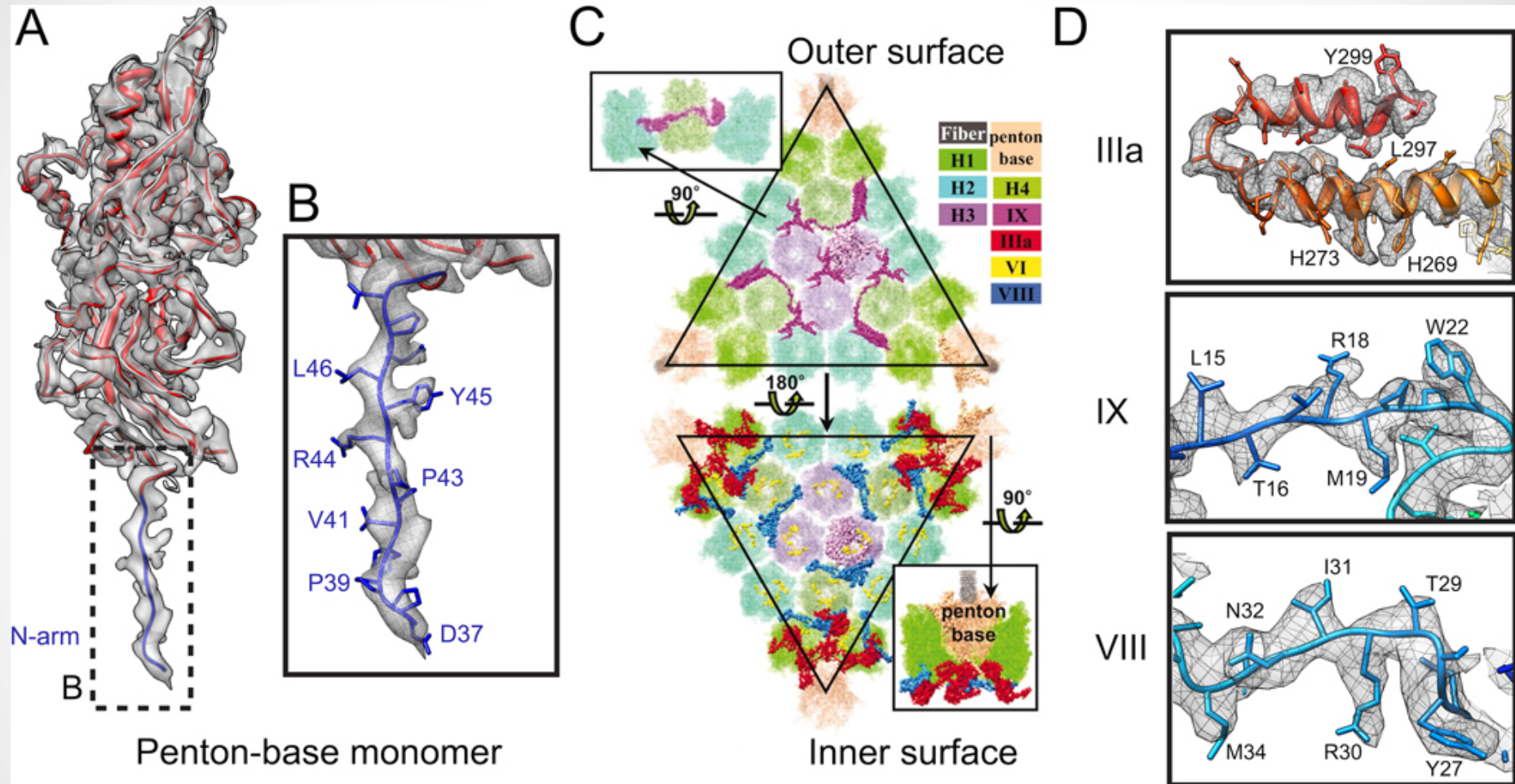


Cryoelectron microscopy and 3D reconstruction of icosahedral viruses

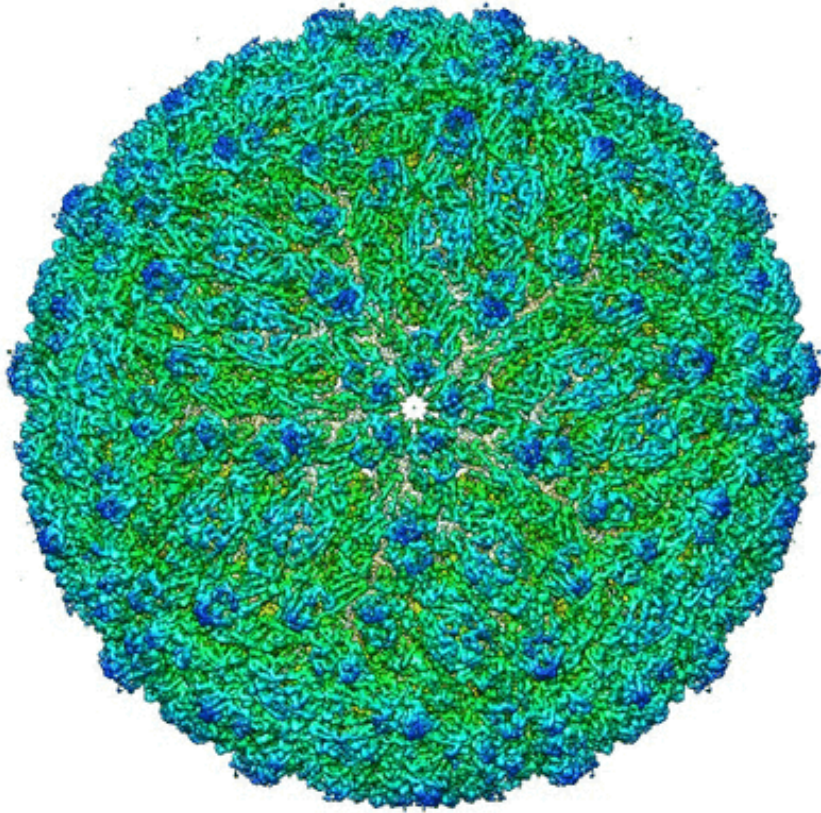
Adenovirus at 3.6 Å



Cryoelectron microscopy and 3D reconstruction of icosahedral viruses

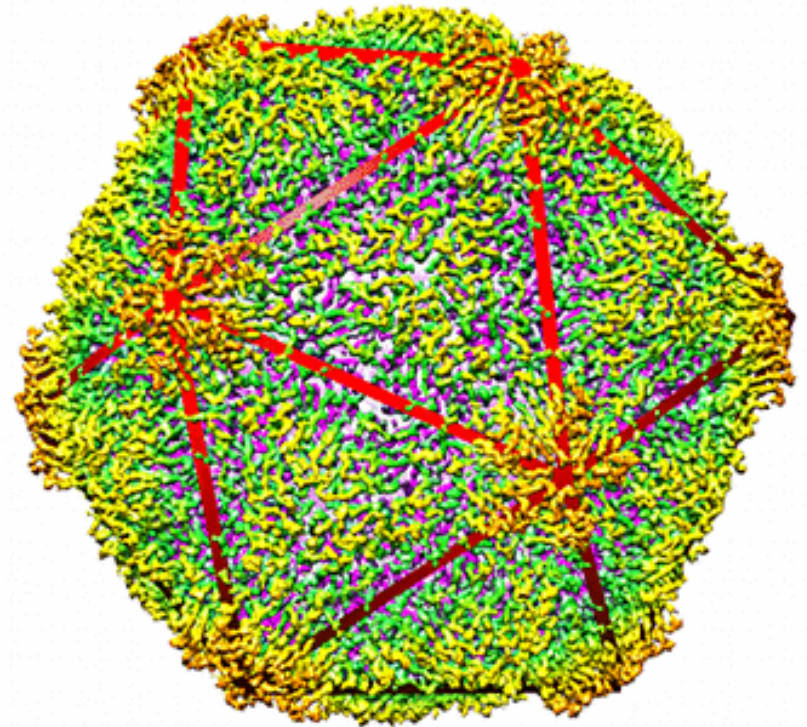


Cryoelectron microscopy and 3D reconstruction of icosahedral viruses



Zika virus at 3.7 Å
EMD8139

Kostyuchenko *et al.*, Nature, 2016



Grapevine fanleaf virus at 2.8 Å
EMD3246

Cryoelectron microscopy and 3D reconstruction of icosahedral viruses

Advantages of electron microscopy

To capture unstable intermediates

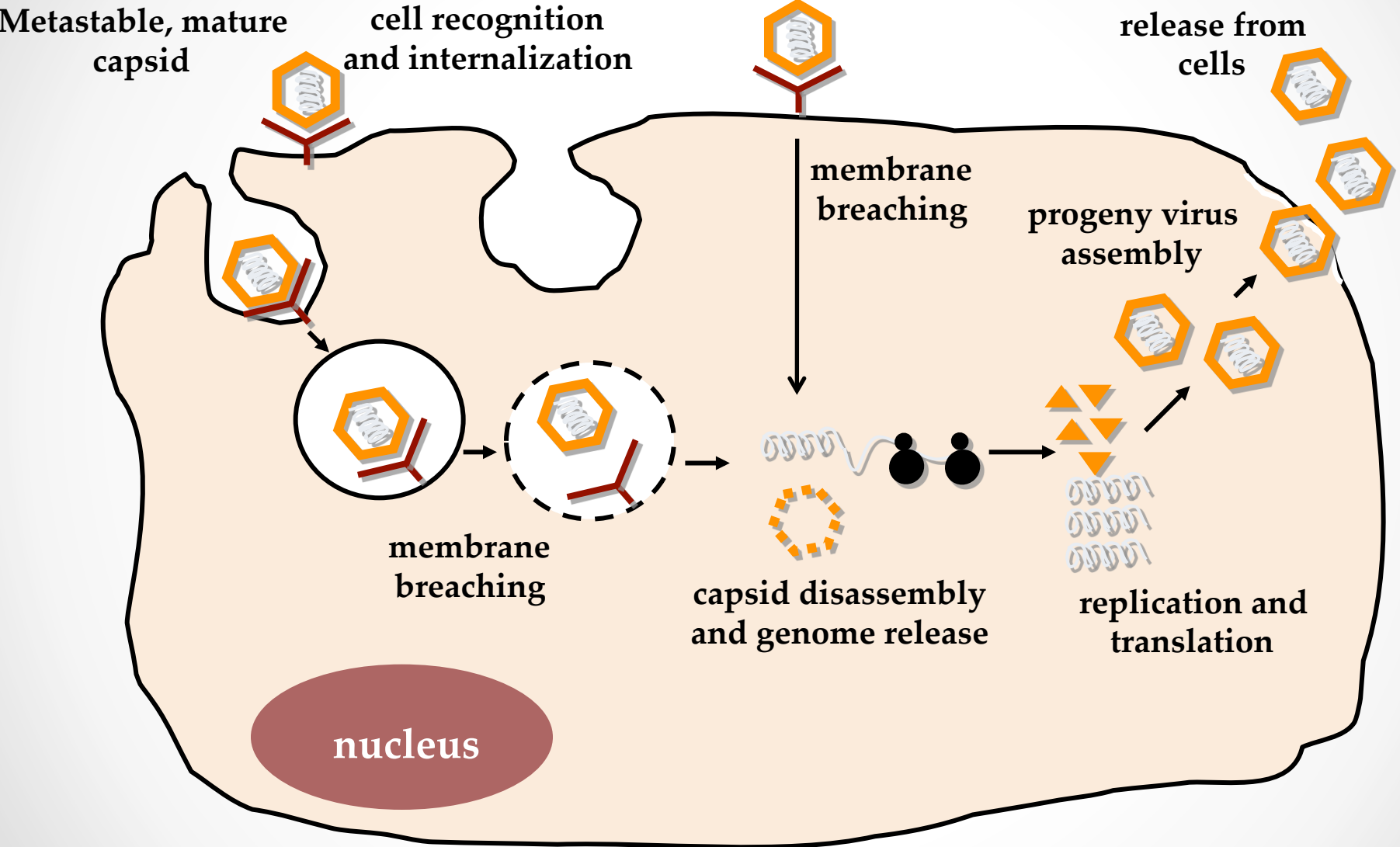
- Difficult to crystallize

- Difficult to freeze crystals

- Data incompleteness

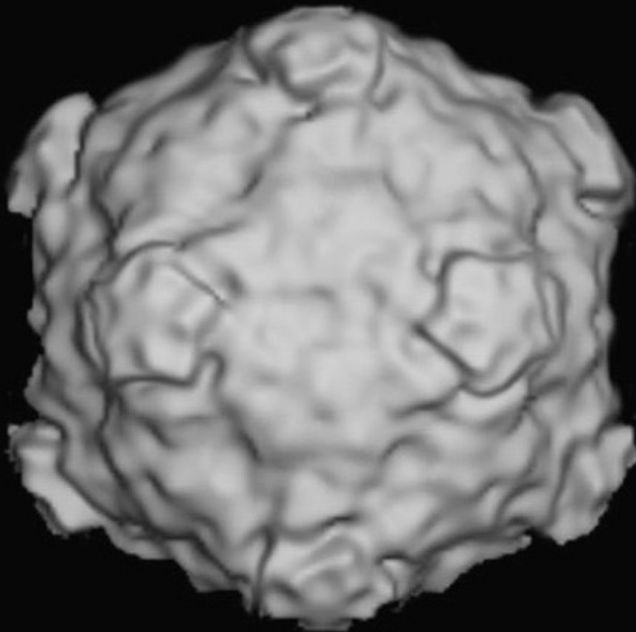
To capture dynamic processes by time-resolved methods

Virus life cycle

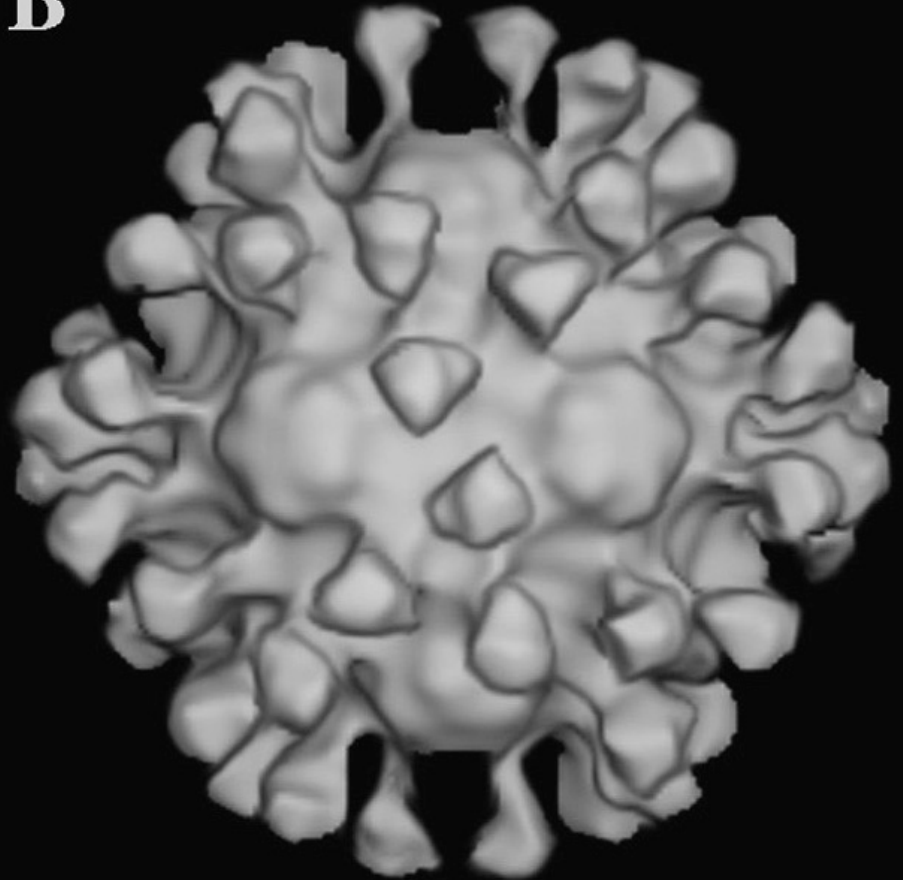


Binding of receptors/antibodies/other molecules to virus particles

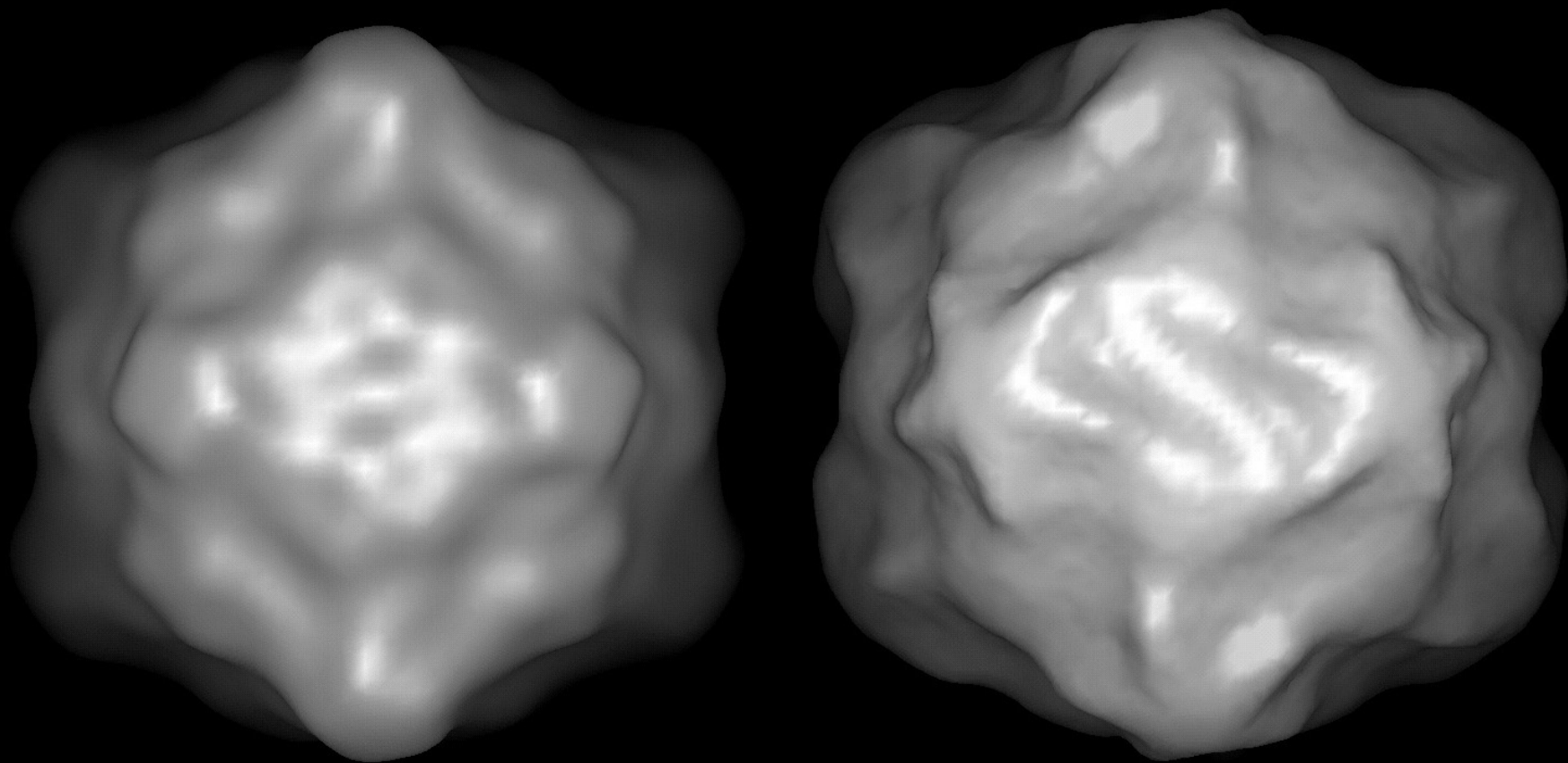
A



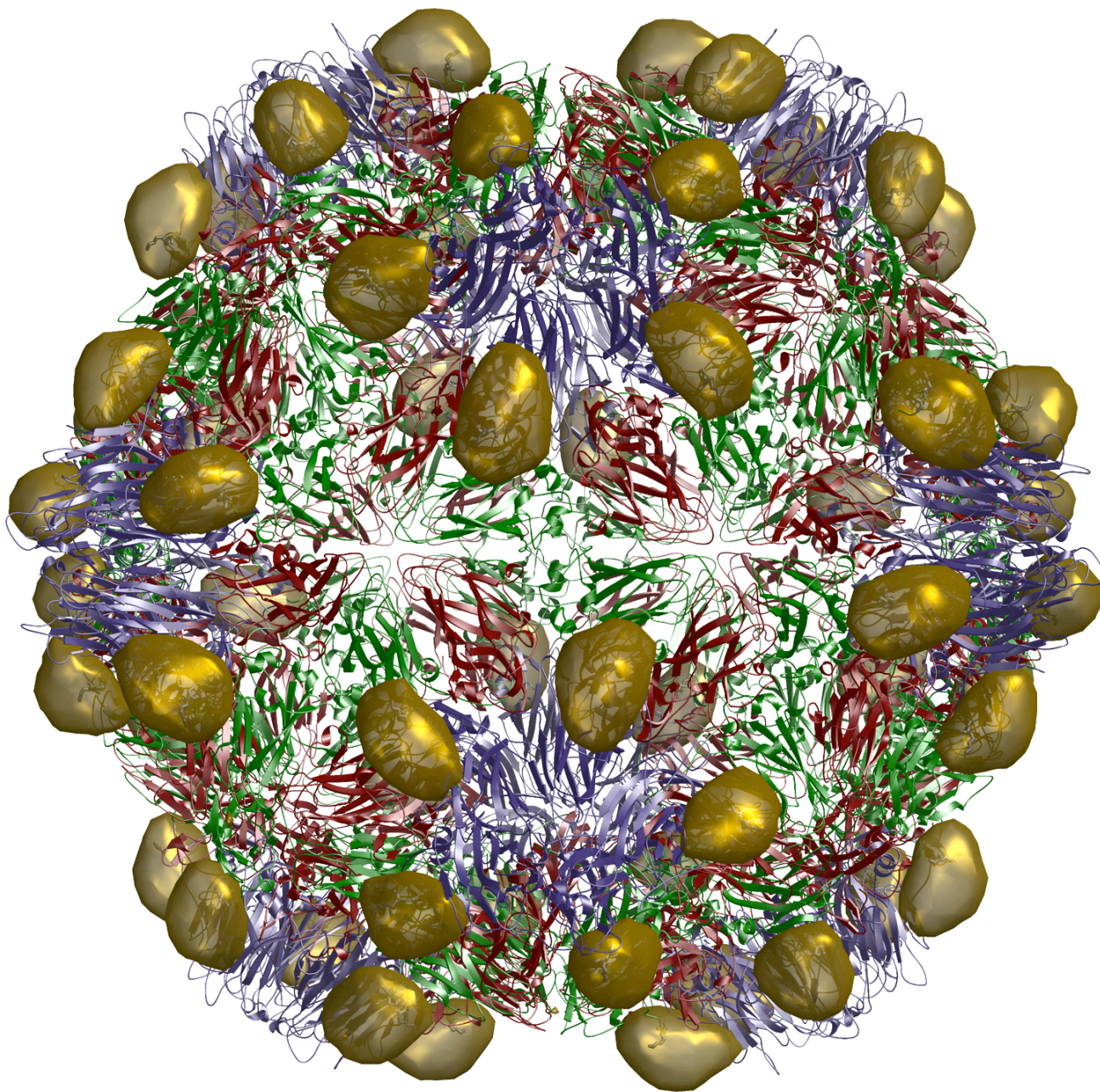
B



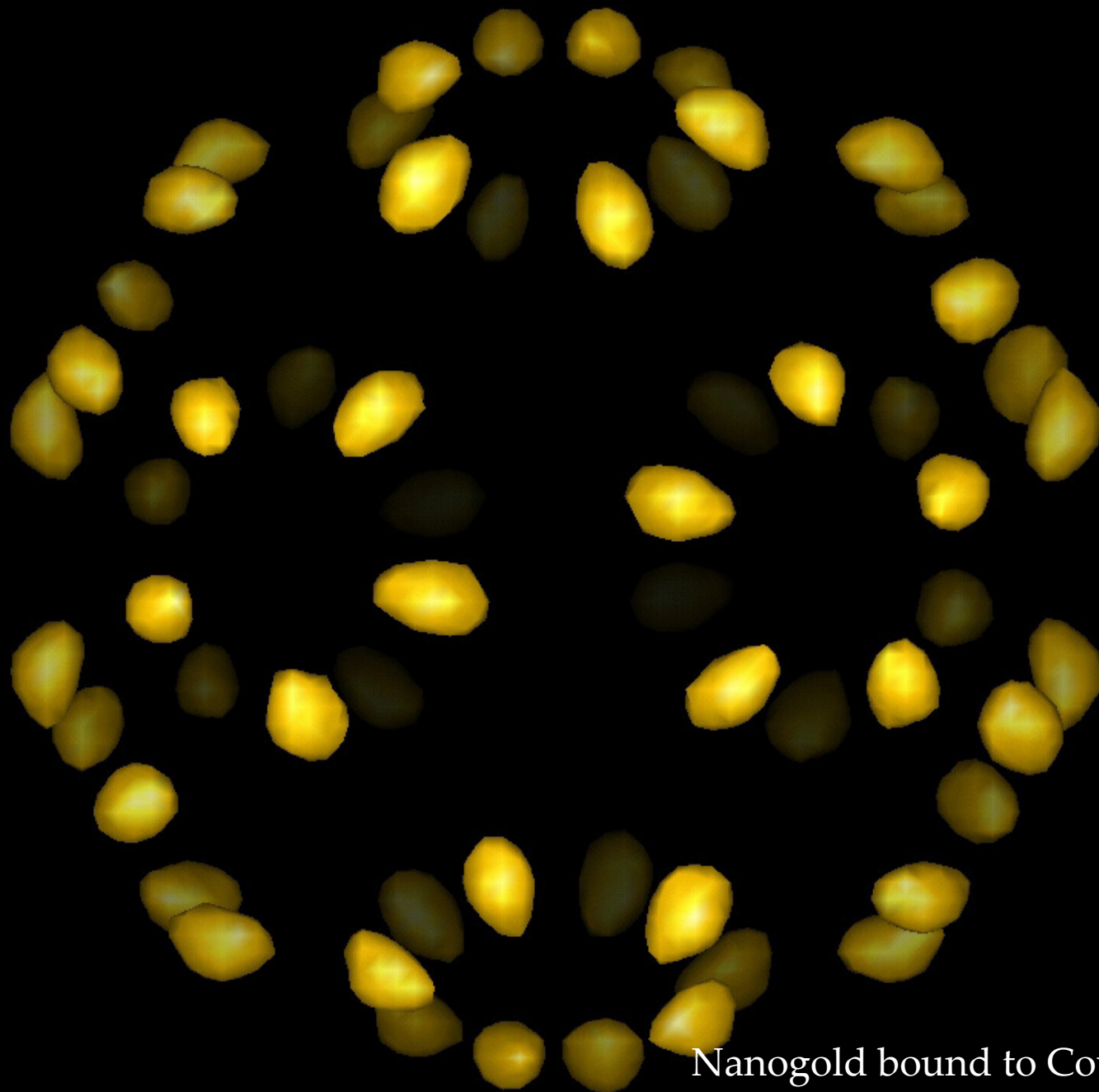
Fab fragments from a monoclonal antibody bound to Cowpea Mosaic Virus
(Wang *et al.*, Nature, 1992)



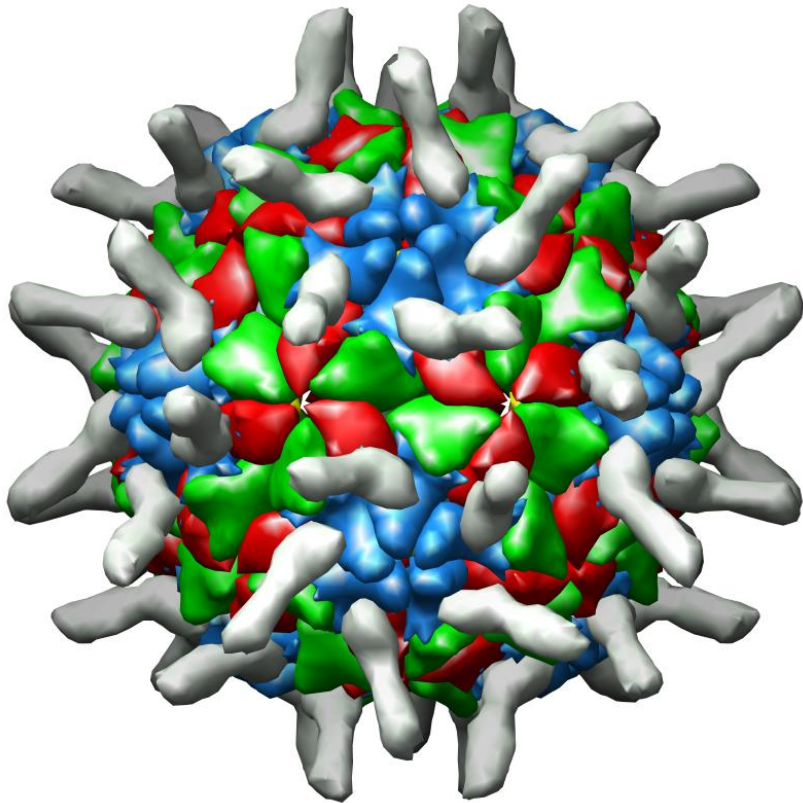
Nanogold bound to Cowpea Mosaic Virus
(Wang *et al.*, Agnew Chem, 2002)



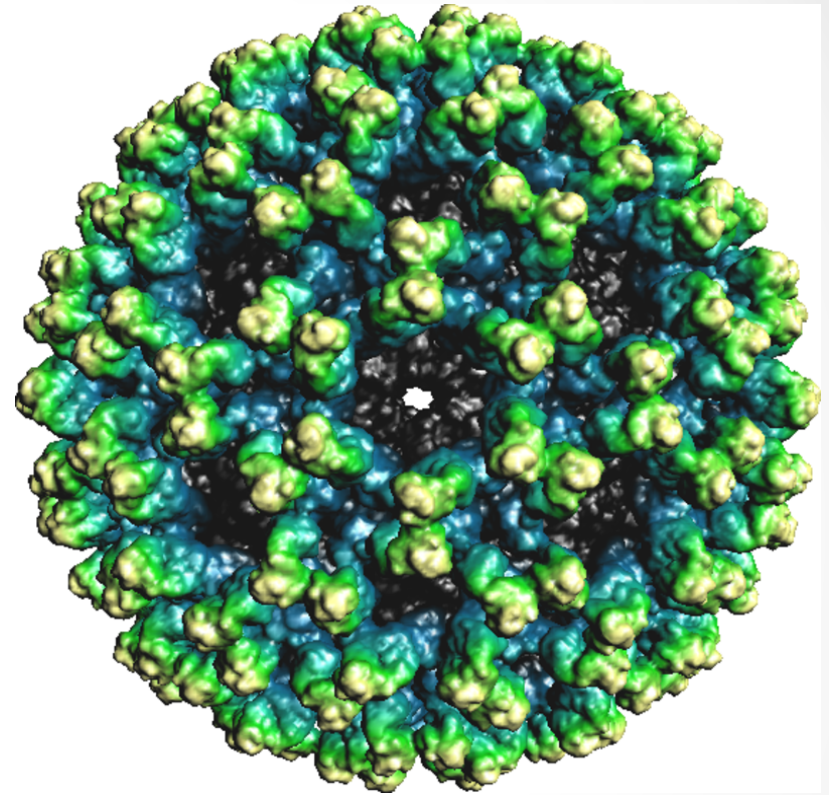
Nanogold bound to Cowpea Mosaic Virus
(Wang *et al.*, *Angew Chem*, 2002)



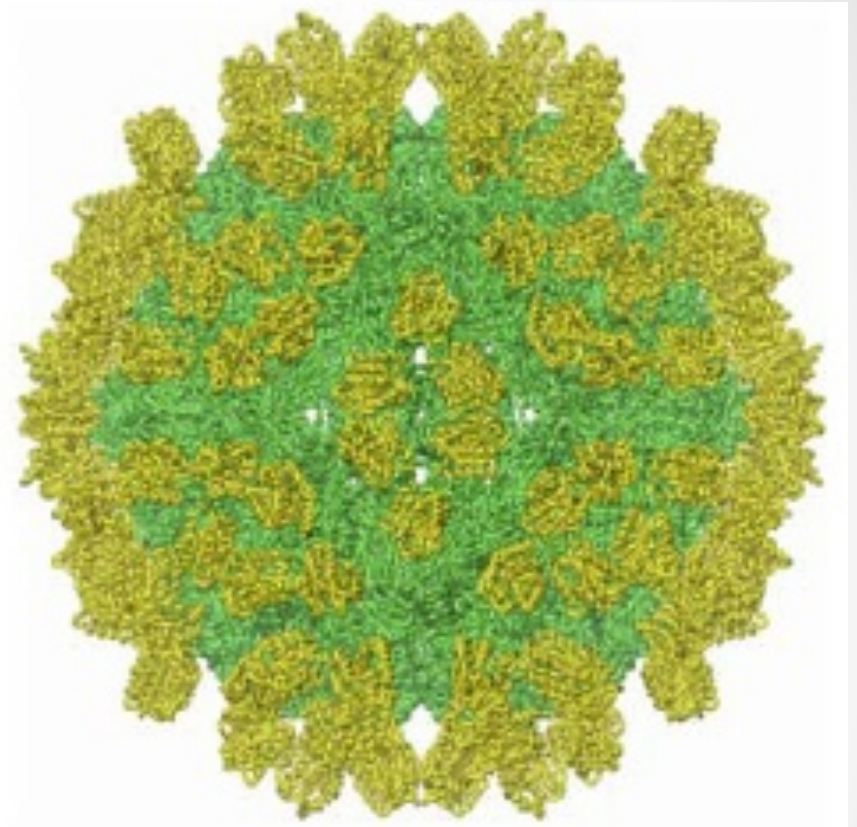
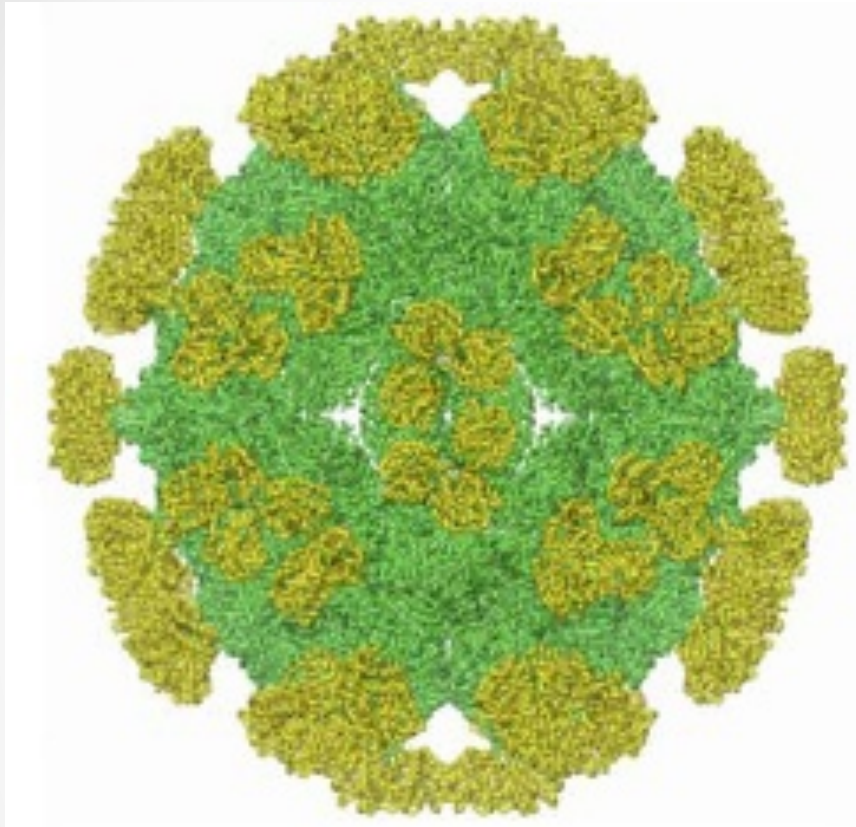
Nanogold bound to Cowpea Mosaic
(Wang *et al.*, Agnew Chem, 2002)



Poliovirus bound to receptor

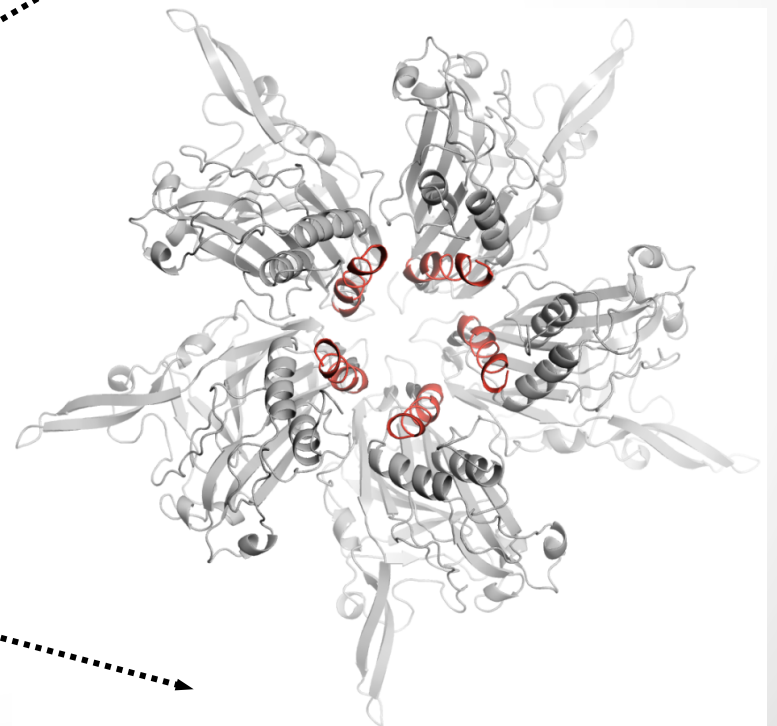
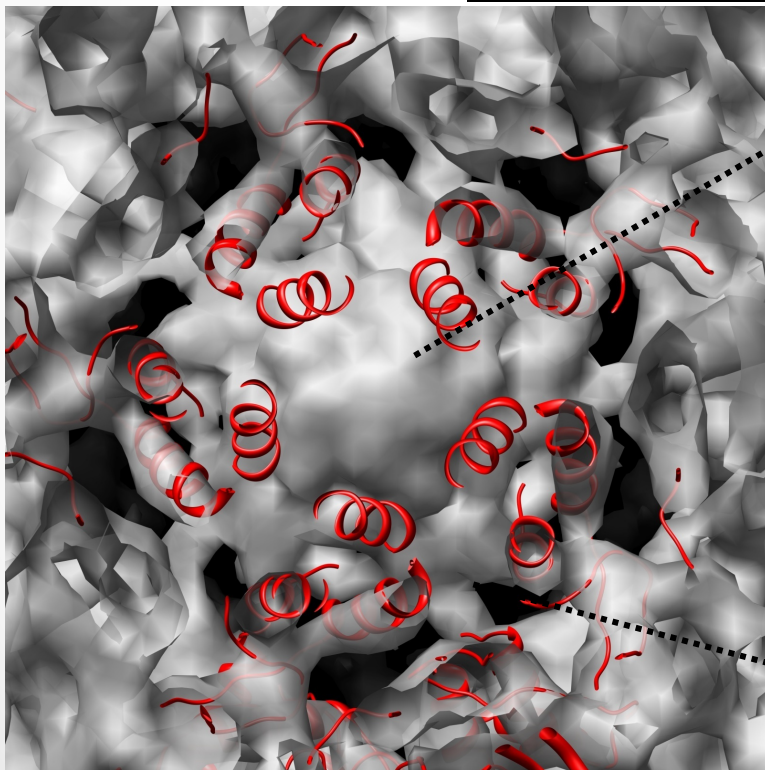
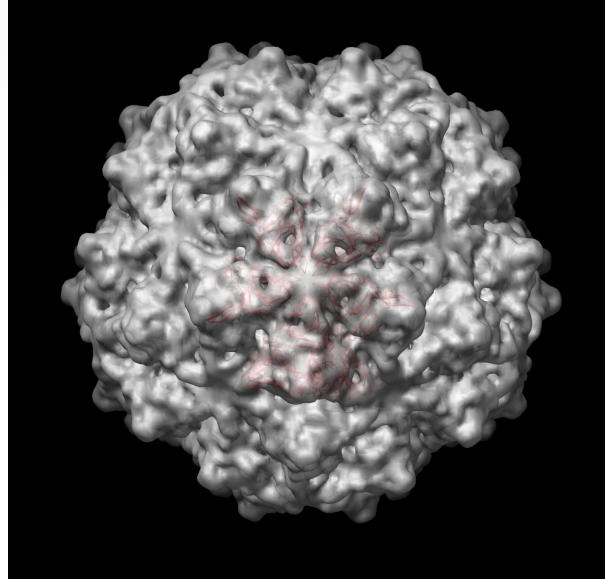


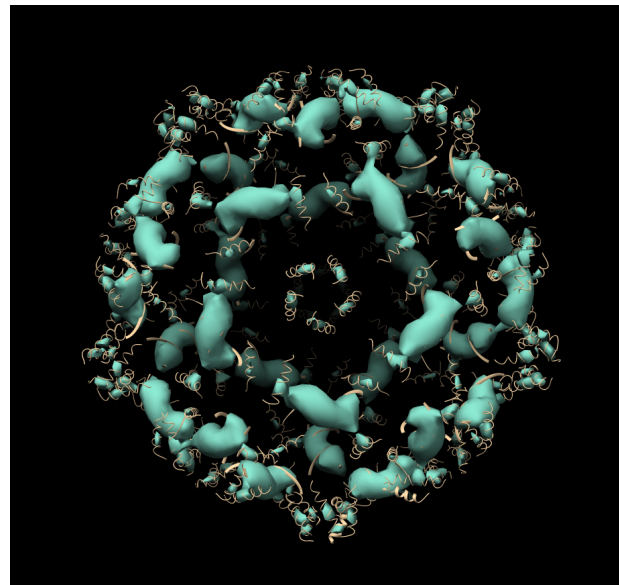
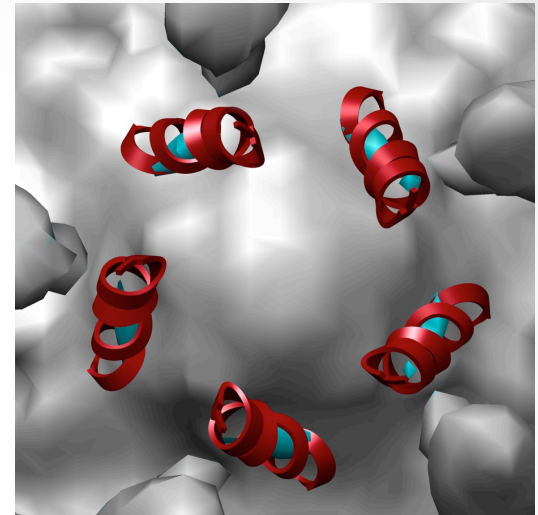
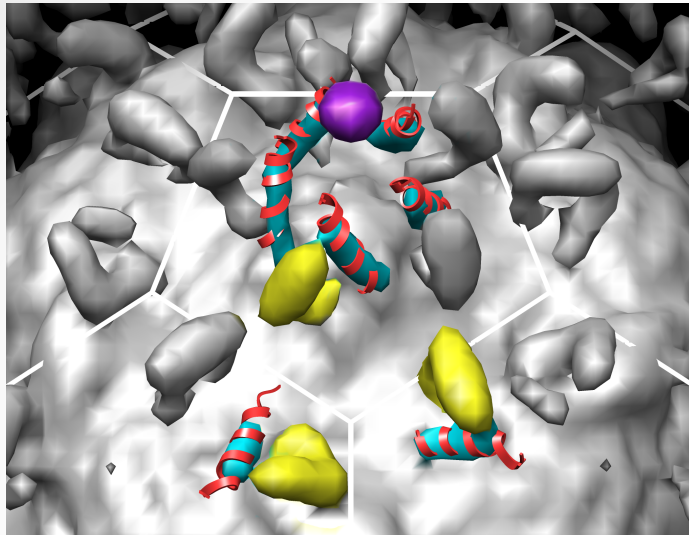
CHIKV bound to antibody



FHV conjugated to anthrax toxin receptor

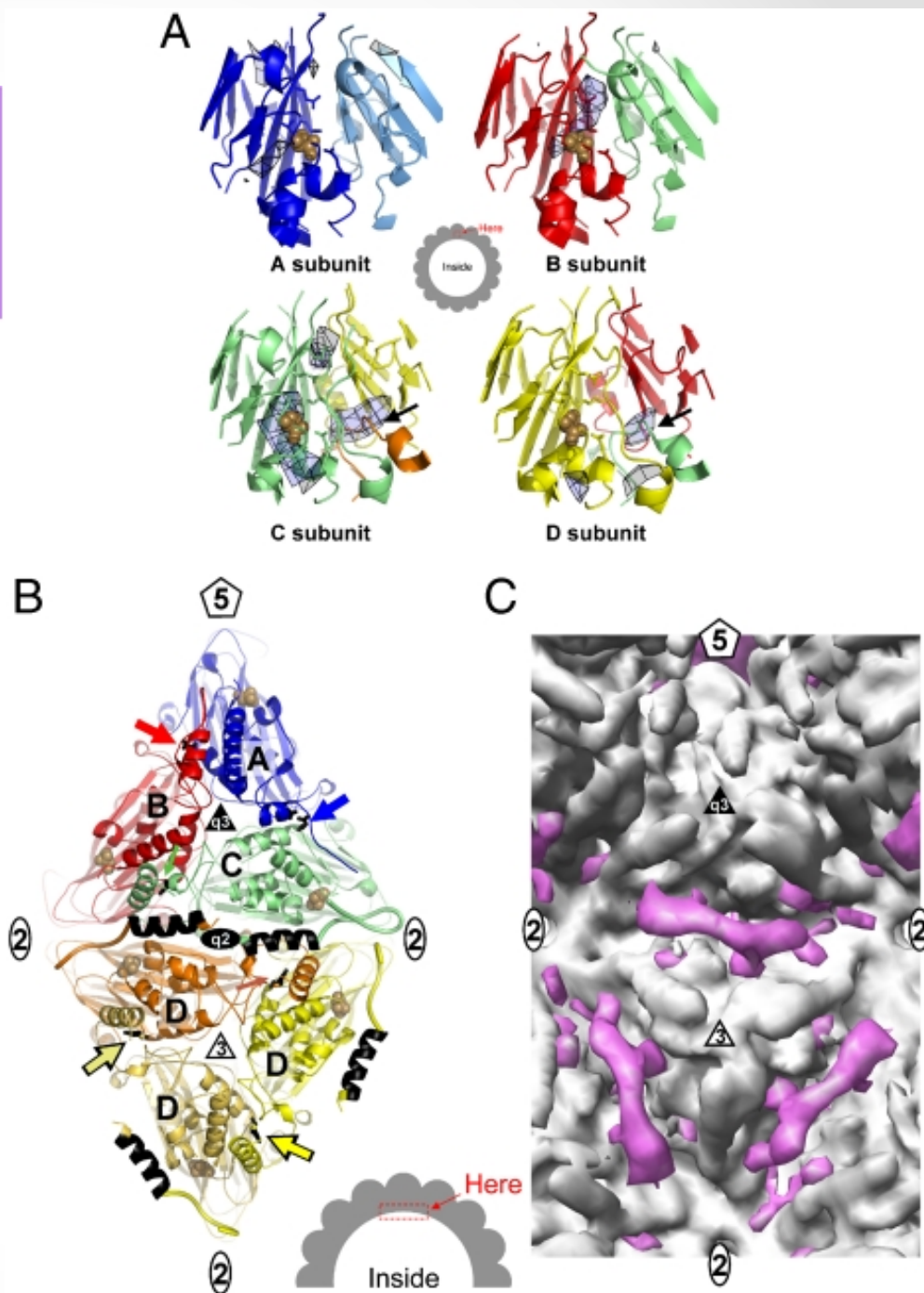
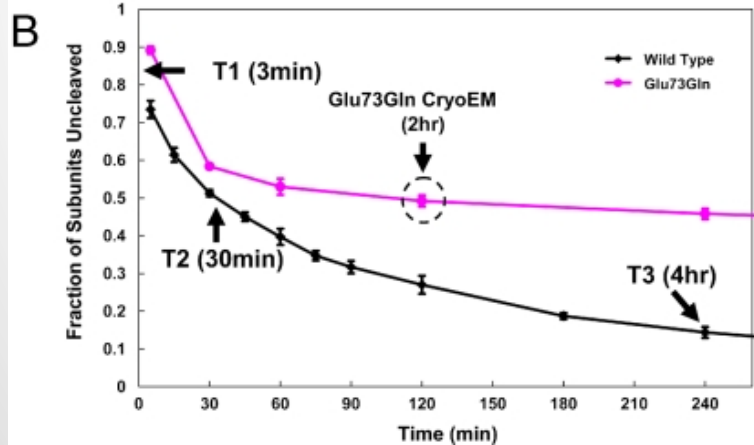
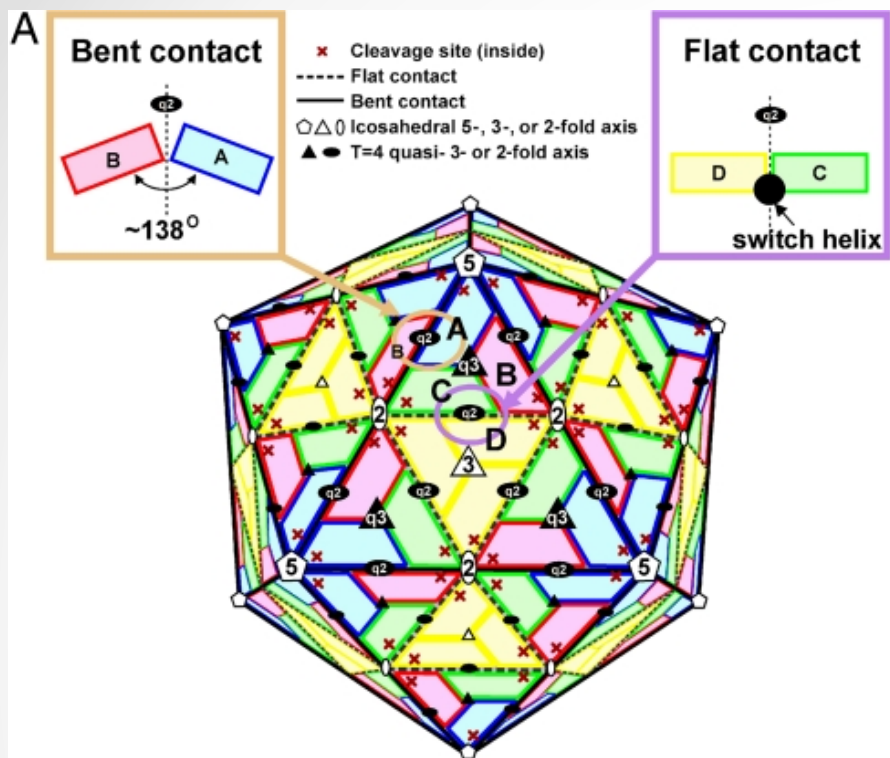
Membrane penetration – effect of quasi-equivalent peptides



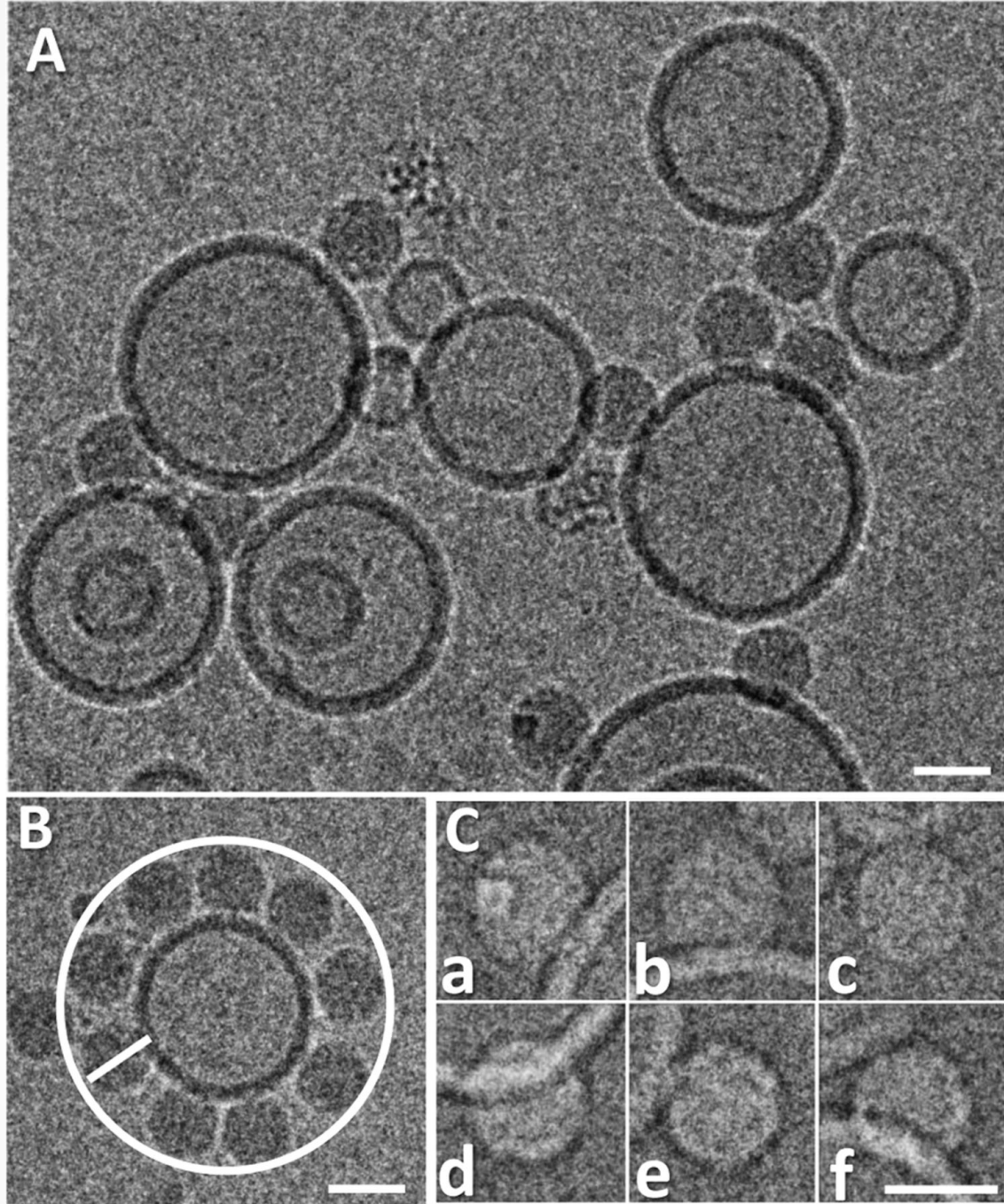


Banerjee *et al*, J Virol, 2009
 Bajaj *et al*, JMB, 2016

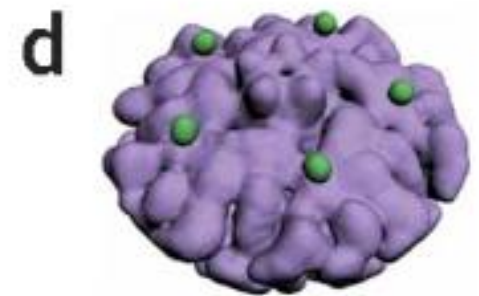
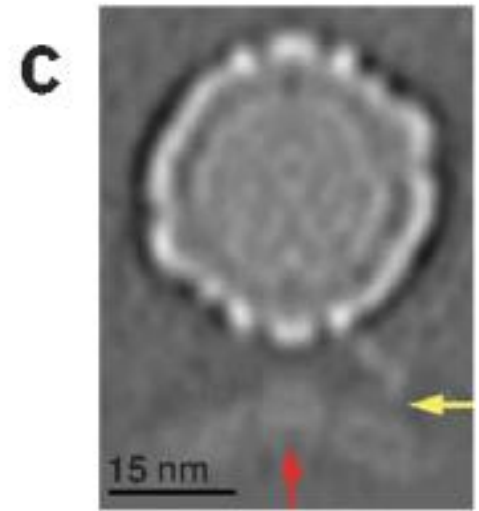
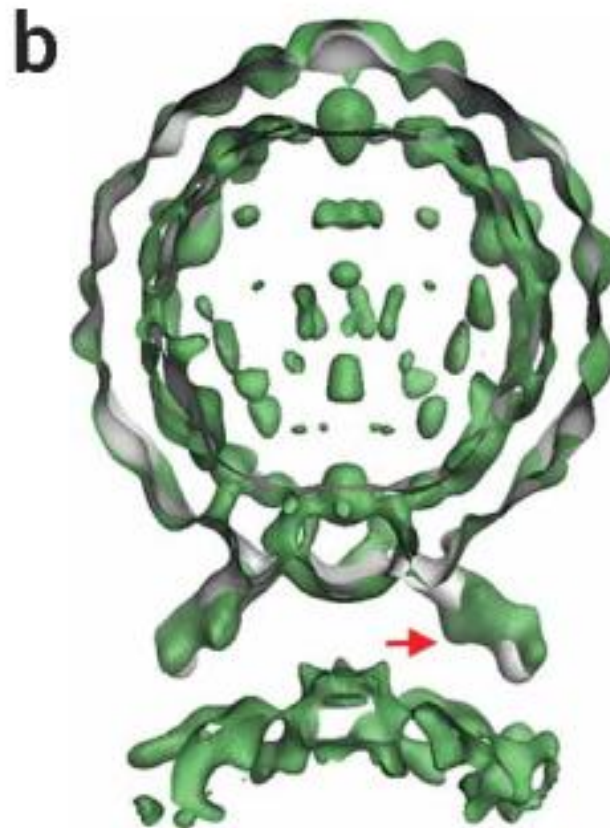
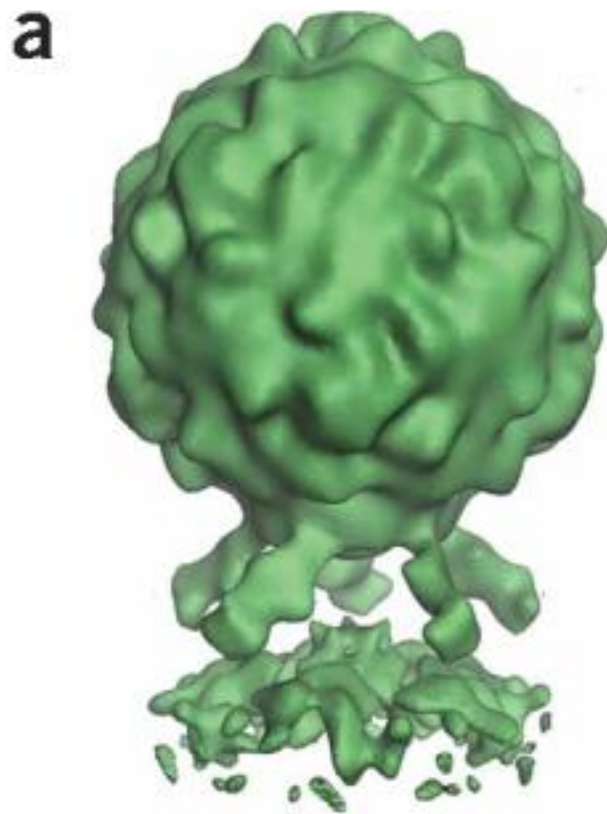
Time-resolved membrane penetration



Membrane interaction

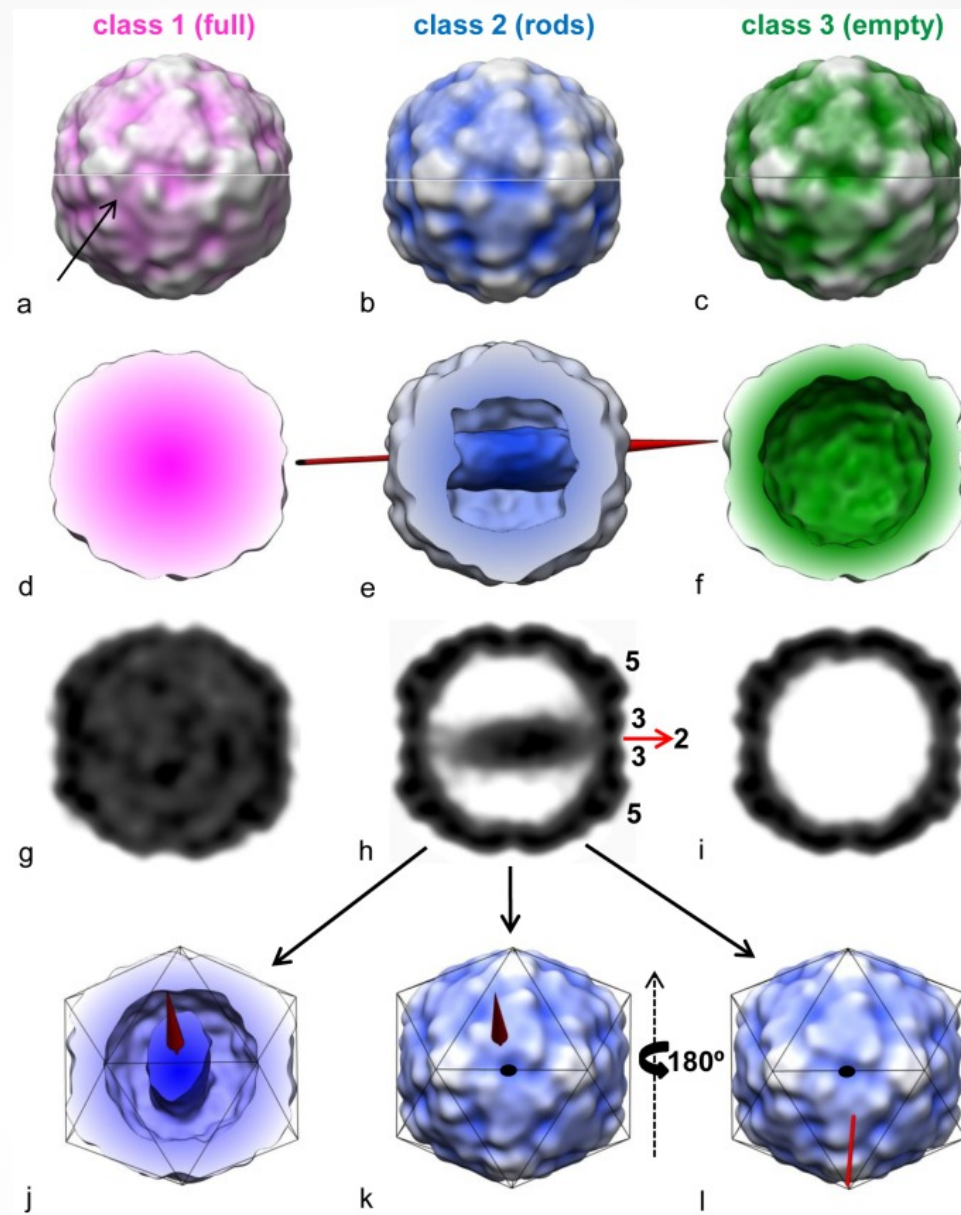


Membrane interaction by HRV2 Kumar *et al.*, JVI, 2014

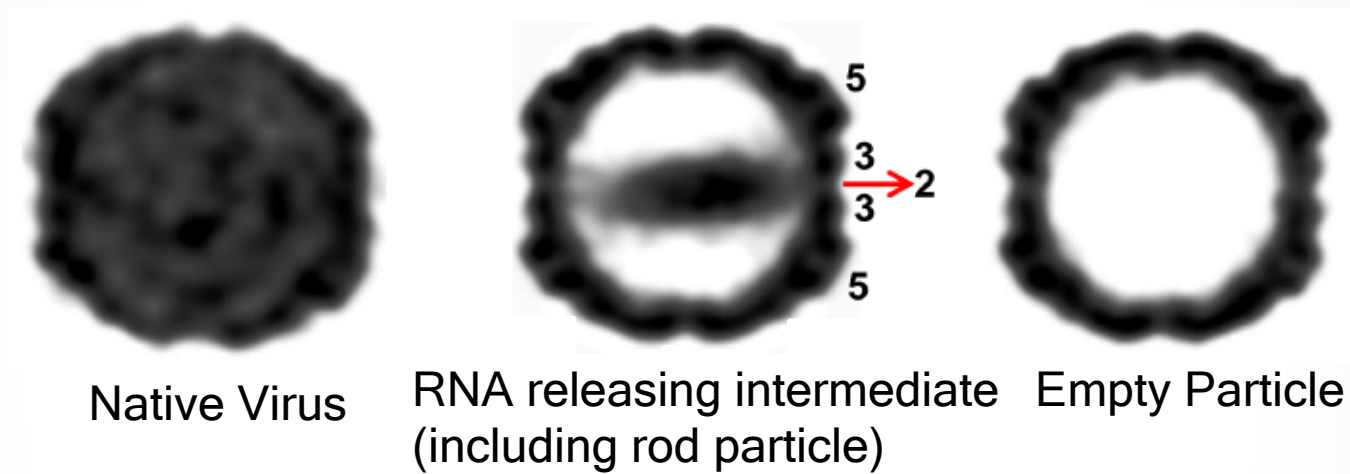


Membrane interaction by poliovirus

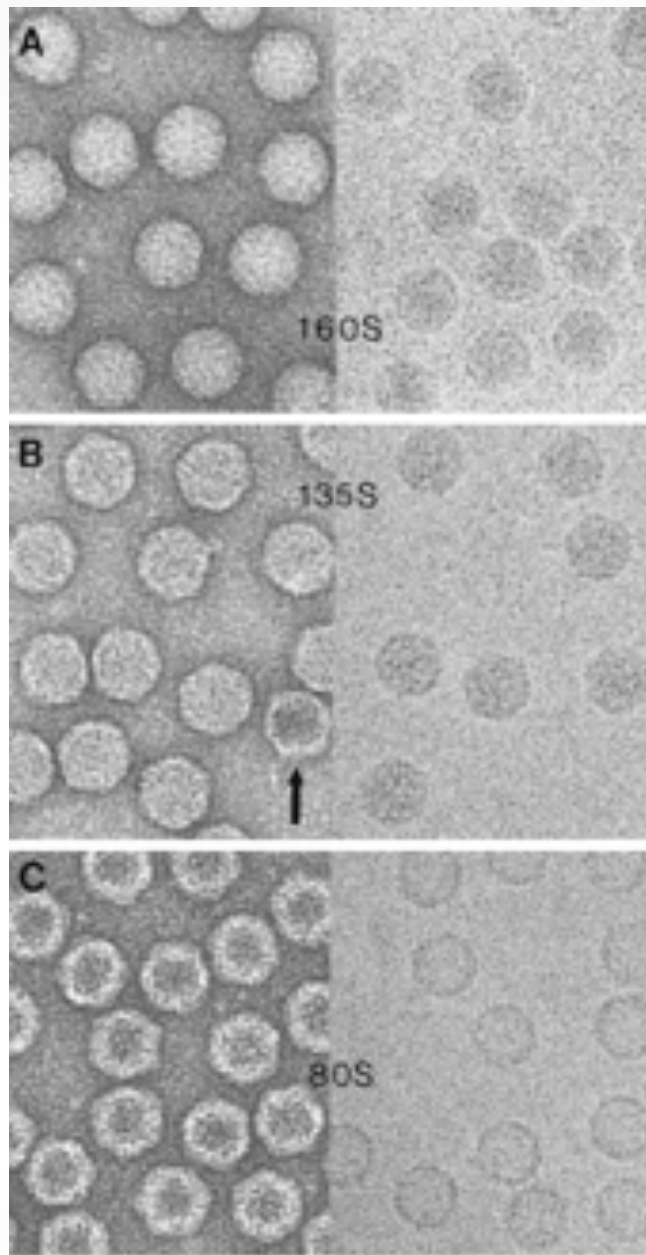
Release of genome (uncoating)



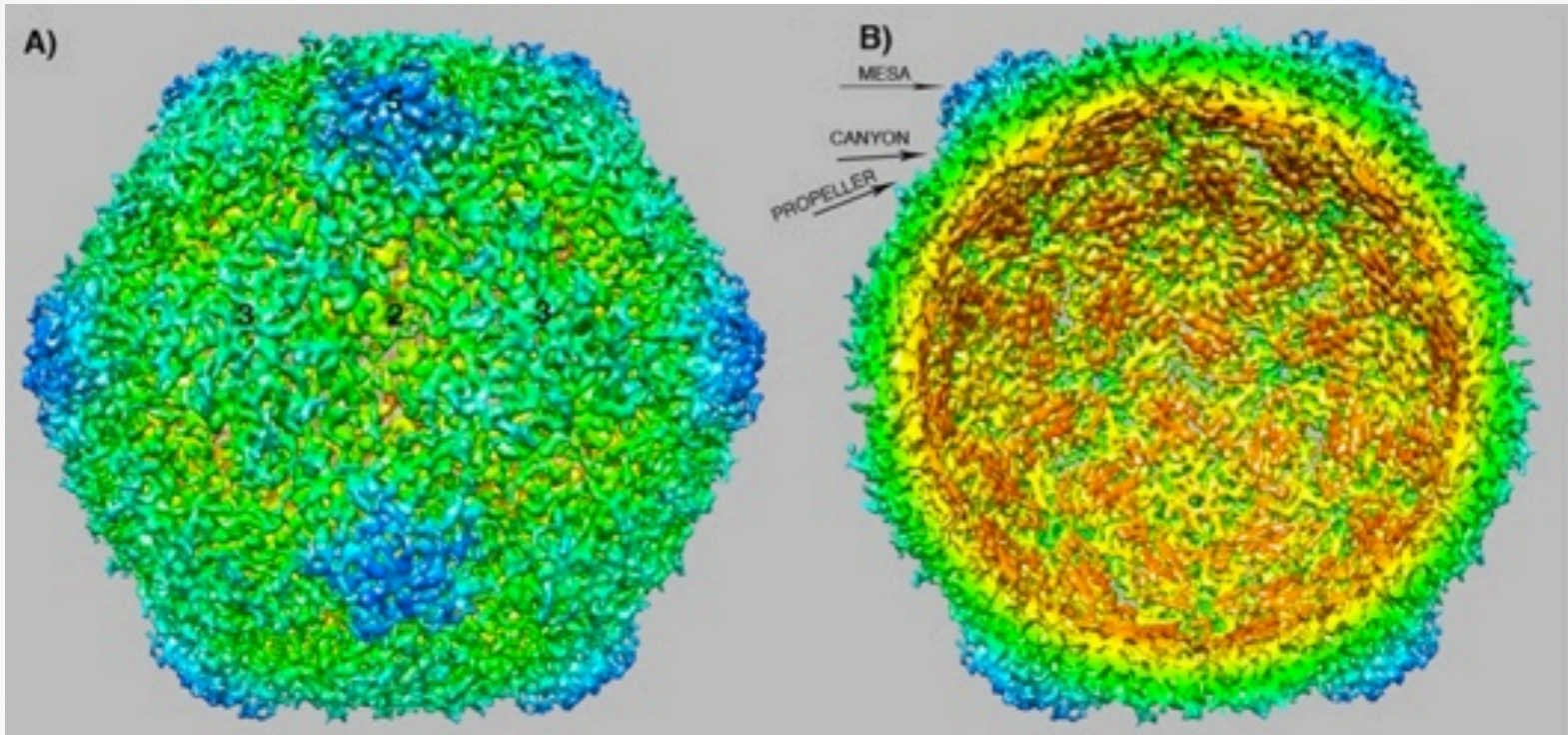
Genome release intermediates of HRV2



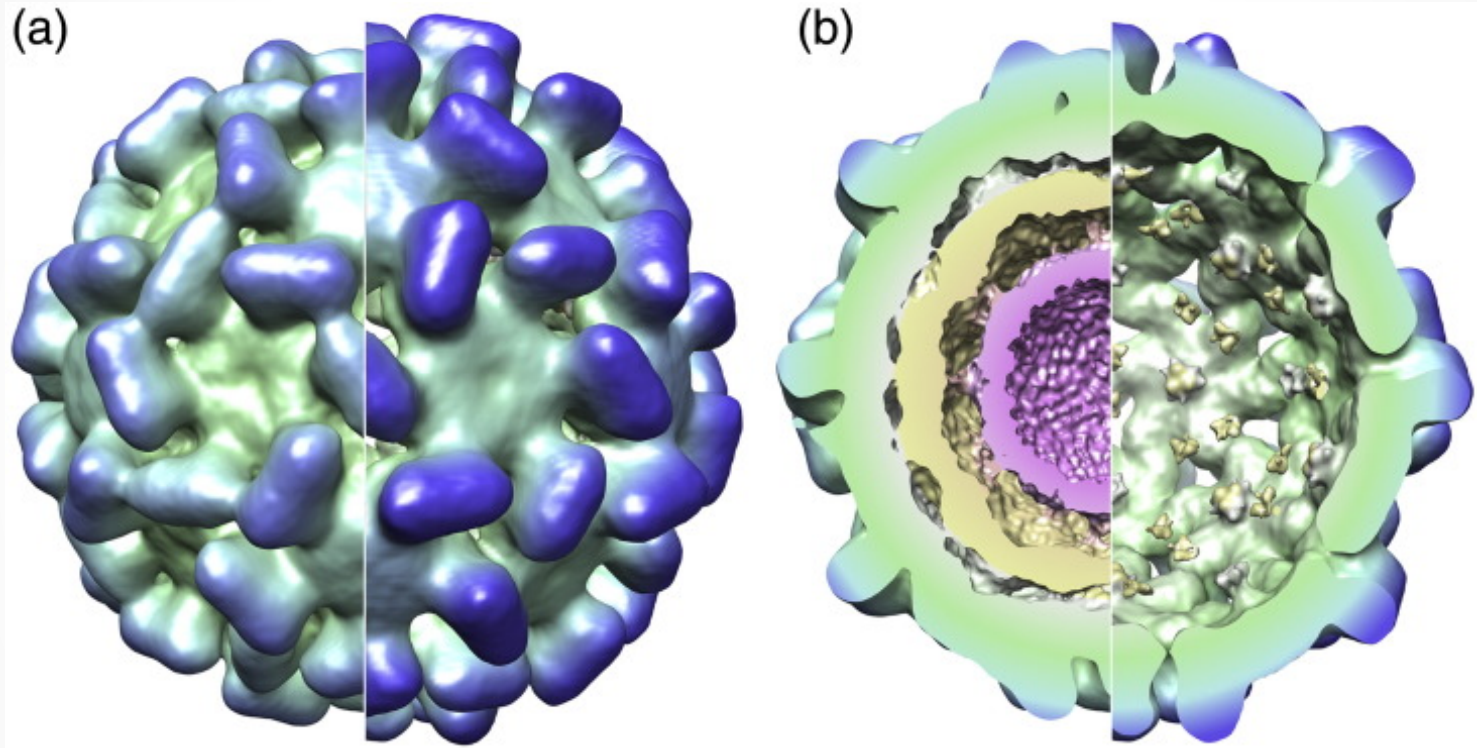
Genome release intermediates of HRV2



Genome release intermediates of poliovirus

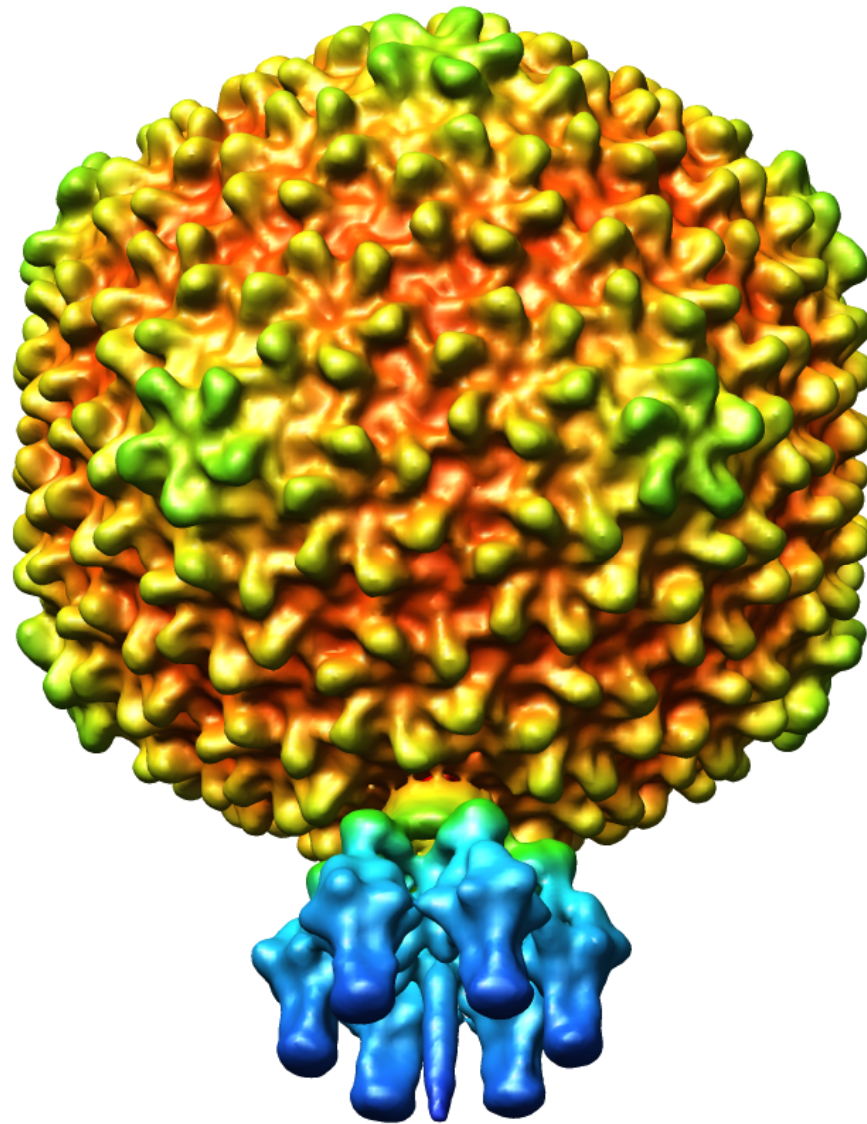


Genome release intermediates of poliovirus

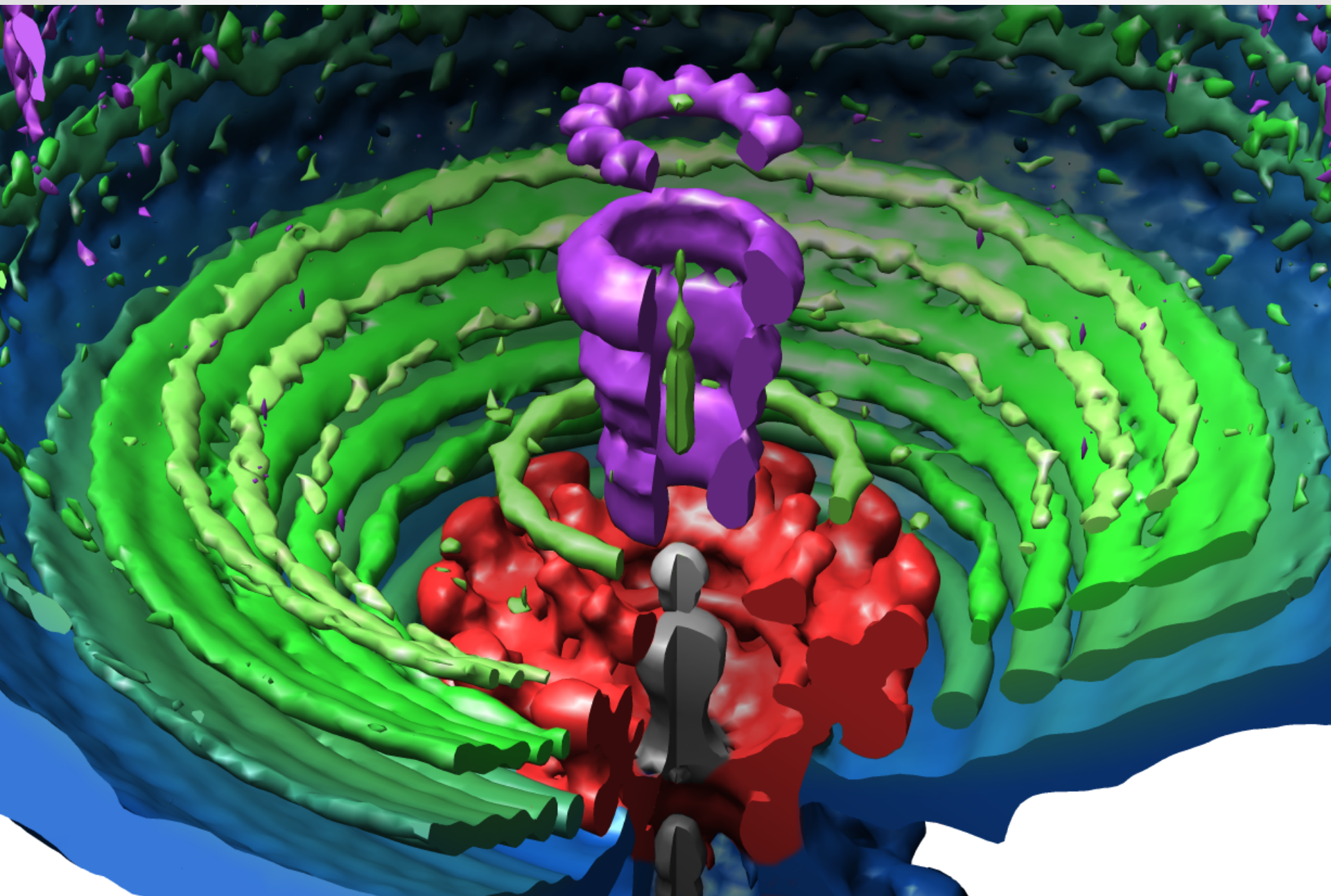


Uncoating intermediate of a plant virus

Mechanism of DNA packaging



Asymmetric reconstruction of P22 bacteriophage



Assembly and maturation

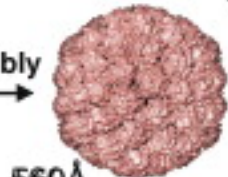
HK97: expression and assembly in *E-coli*

Capsid proteins
(gp5) as
capsomers



Protease
(gp4) ~ 60x

Assembly



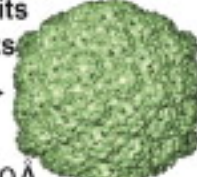
560Å
Prohead I
7Å cryoEM
reconstruction

Proteolysis
of the
 Δ -domain
and the
protease

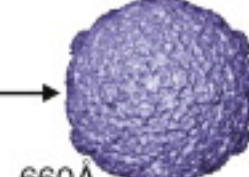


560Å
Prohead II
3.6Å

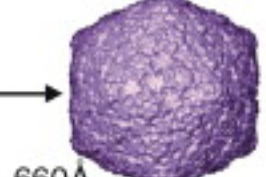
Maturation:
expansion
and subunits
cross-links



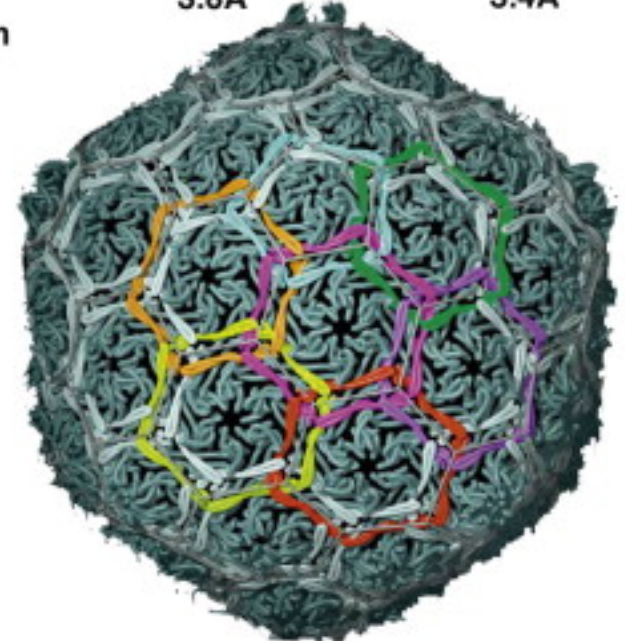
610Å
EI I~III
15Å cryoEM
reconstruction



660Å
EI IV
3.8Å

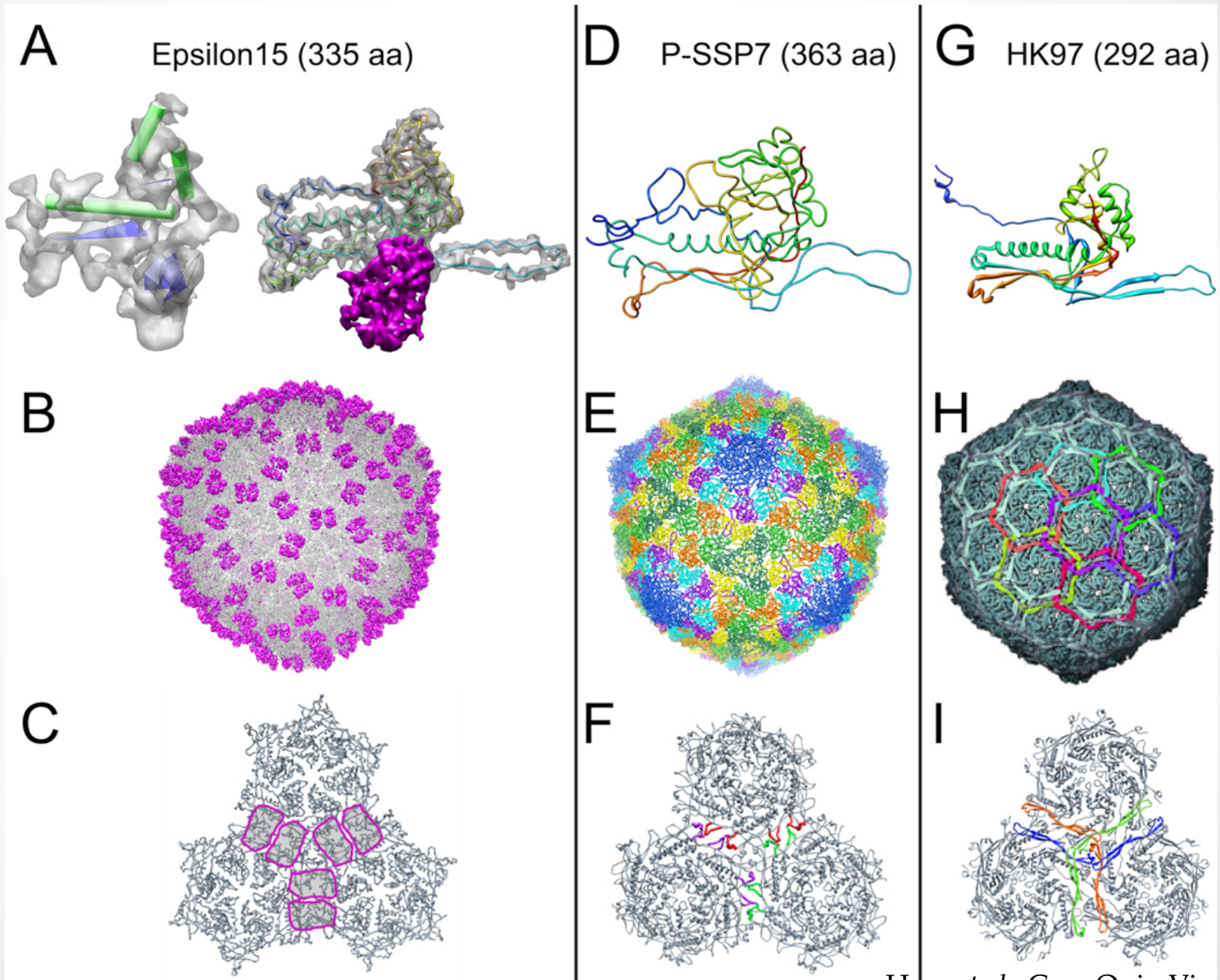


660Å
Head II
3.4Å

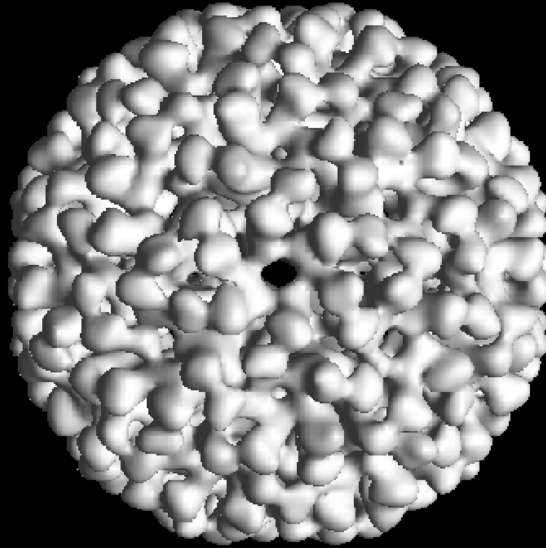


Current Opinion in Structural Biology

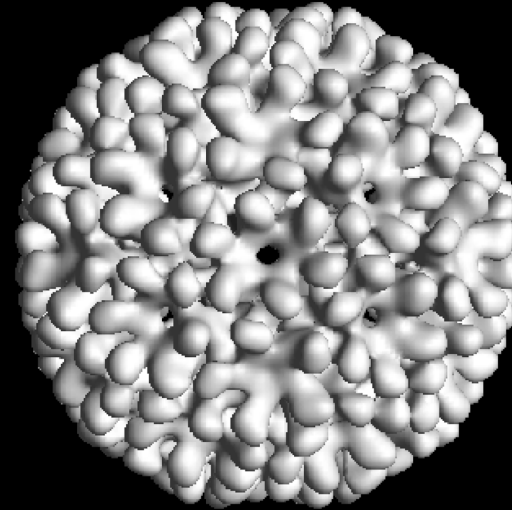
Cryoelectron microscopy and 3D reconstruction of icosahedral viruses



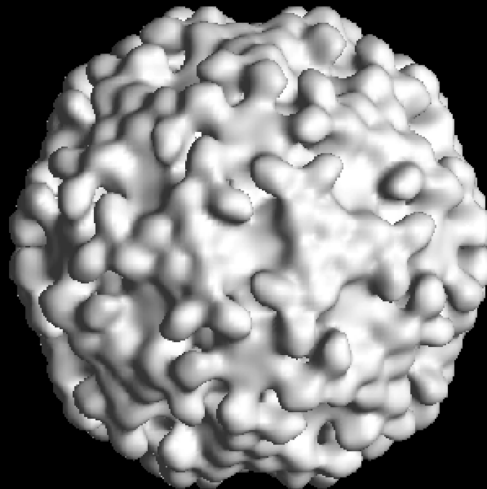
procapsid



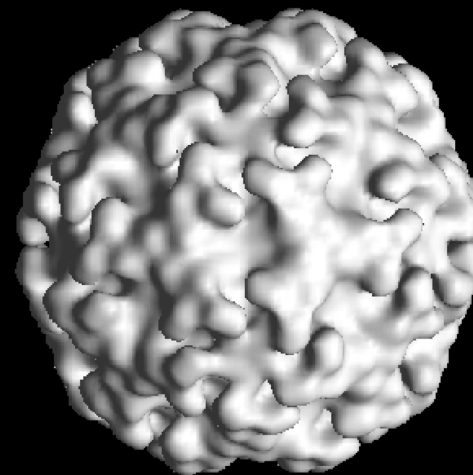
pH5.8 intermediate



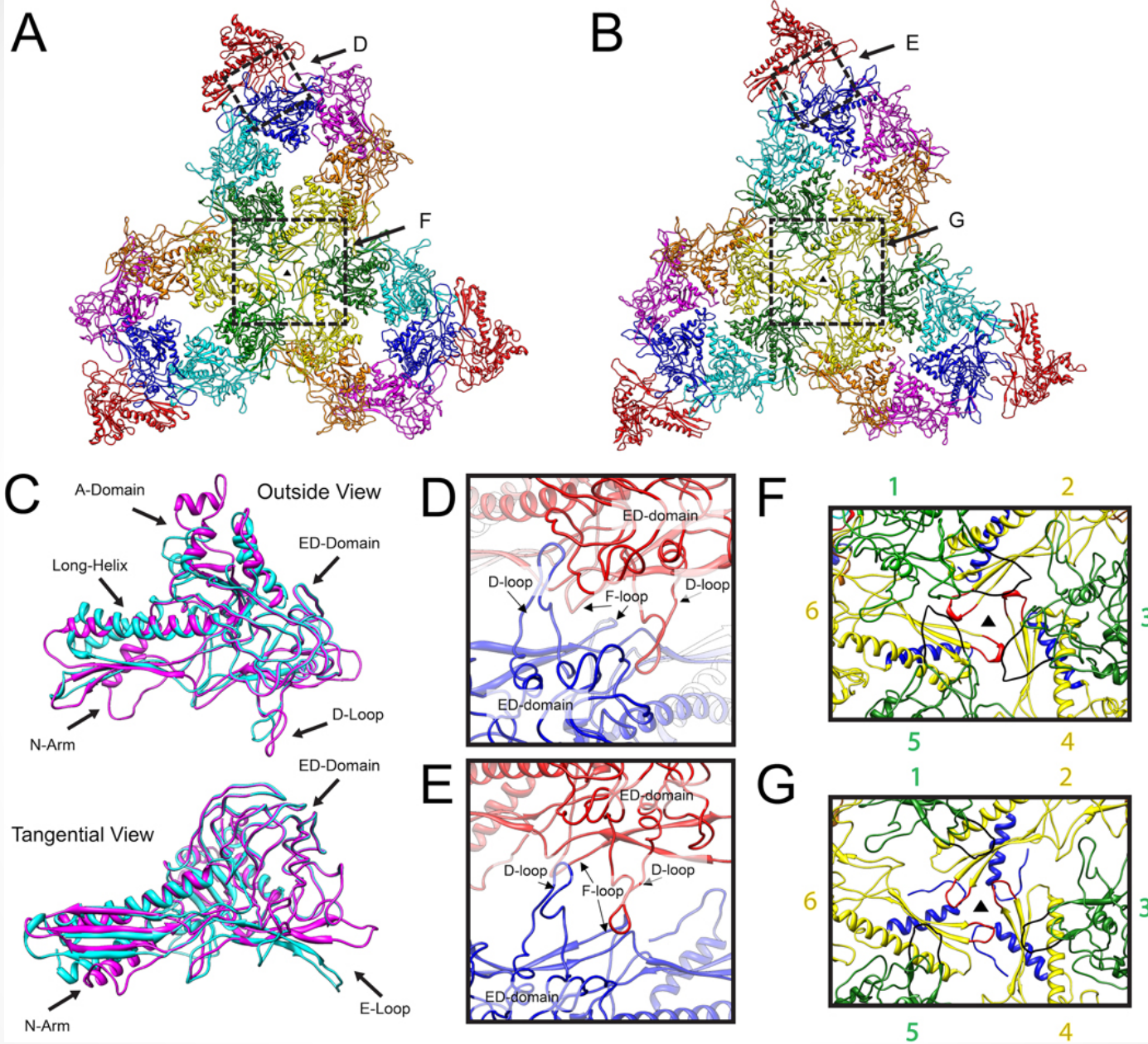
pH5.5 intermediate



capsid



Maturation of N ω V procapsid



Maturation of P22 procapsid

References

Procedures for three-dimensional reconstructions of spherical viruses by Fourier synthesis from electron micrographs. R A Crowther. Philos Trans R Soc Lond B Biol Sci. 1971. 261 (837): 221-30

The making and breaking of symmetry in virus capsid assembly: glimpses of capsid biology from cryoelectron microscopy. Alasdair C. Steven, Benes I Trus, Frank P. Booy, Naiqian Cheng, Adam Zlotnick, Jose R. Caston, and James F. Conway. FASEB J 1997; 734-741

Adding the third dimension to virus life cycles: three-dimensional reconstruction of Icosahedral viruses from cryo-electron micrographs. T. S. Baker, N. H. Olson and S. D. Fuller. Microbiol Mol Biol Rev. 1999, 862-922

Multidisciplinary studies of viruses: The role of structure in shaping the questions and answers. John E. Johnson. *J Struct Biol.* 2008; 163(3): 246–253.

Near-atomic-resolution cryo-EM for molecular virology. Corey F. Hryc, Dong-Hua Chen, and Wah Chiu. Curr Opin Virol. 2011; 1(2): 110–117

References

Structure Determination of Icosahedral Viruses Imaged by Cryo-electron Microscopy. Robert S. Sinkovits and Timothy S. Baker. RSC Biomolecular Sciences, Structural Virology (Chapter 5), published by Royal Society of Chemistry, 2011

Reconstructing virus structures from nanometer to near-atomic resolutions with cryo-electron microscopy and tomography. Juan Chang, Xiangnan Liu, Ryan H. Rochat, Matthew L. Baker, and Wah Chiu. Adv Exp Med Biol. 2012 ; 726: 49–90.

Principles of Virus Structural Organization. B.V. Venkataram Prasad and Michael F Schmid. Adv Exp Med Biol. 2012 ; 726: 17–47

Photo credit: Internet sources

EMDB

VIPERdb